Mohamed Khider University of Biskra
Faculty of Science and Technology
Department of Mechanical Engineering

MASTER DISSERTATION

Field : Sciences et Techniques
Sector: Metallurgy
Specialty: Metallurgy Engineering

Ref.:

Presented and supported by:

DJIMAOUI Nour El Imane

On : June, 28, 2022

Laser and TIG welding of low carbon steel for LPG car tank industry.

Jury:

Dr.	MESSAOUDI Salim	MCB	University of Biskra	President
Dr.	BENTRAH Hamza	MCA	University of Biskra	Examiner
Pr.	BOUMERZOUG Zakaria	Pr	University of Biskra	supervisor

Academic year: 2021- 2022

Université Mohamed Khider de
Biskra
Faculté des Sciences et de
la Technologie
Département de Génie Mécanique

MÉMOIRE DE MASTER

Domaine : Sciences et Techniques
Filière : Métallurgie
Spécialité : Génie Métallurgique

Réf. : Entrez la référence du document

Présenté et soutenu par :

DJIMAOUI Nour El Imane

Le : mardi 28 juin 2022

Soudage laser et TIG d'acier à faible pourcentage de carbone pour l'industrie des réservoirs GPL.

Jury :

Dr.	MESSAOUDI Salim	MCB	Université de Biskra	President
Dr.	BENTRAH Hamza	MCA	Université de Biskra	Examinateur
Pr.	BOUMERZOUG Zakaria	Pr	Université de Biskra	Encadreur

Année universitaire : 2021 - 2022

DEDICATION

First of all, I would like to thank ALLAH the Almighty and Merciful, who gave us the strength and patience to accomplish this modest work.

To Djimaoui family… My parents, brothers, sisters

I dedicate my dissertation work to DJIMAOUI family who always encourage me with passion and endless support. I am so lucky to have such family Love me so much and believe on me.

To my friends

I dedicate my dissertation work to my friends ***(Nadia, Oumnia, Youssera, Jannat, Safa)*** *Thank you very much for all your support, for the moments of joy and sorrow shared.*

To my promotion **Metallurgy Engineering (2021-2022)**

This work is dedicated to you and may ALLAH fill you with his blessings.

To all my teachers

From those who taught me to write my name, as a sign of deep gratitude and recognition

To myself

Finally, I dedicate this dissertation to myself ***DJIMAOUI Nour El Imane*** *who worked hard during the 5 past years and during the realisation of this dissertation*

ACKNOWLEDGMENTS

I warmly thank my supervisor, professor ***BOUMERZOUG Zakaria*** *who offered me this research topic and also its availability throughout this academic year.*

*I would like to thank the members of the jury (****Dr. MESSAOUDI Salim*** *and* ***Dr. BENTRAH Hamza****) who assessed my research work.*

I thank the staff of the ***metallurgy laboratory*** *of mechanical engineering department.*

I also thank ***PETROGEL BATNA*** *industrial establishment for his contribution to release this work.*

Special thanks to ***Dr. DJIMAOUI Toufik*** *for his help throughout realization this dissertation.*

Table of content

List of tables

Chapter II

Chapter III

List of figures

Chapter I:

Chapter II:

Chapter III:

Chapter IV:

General Introduction

Welding is a fabrication process that joins materials, usually metals or thermoplastics, by using high heat to melt the parts together and allowing them to cool, causing fusion. Welding is used in many fields of industry.

Steels can be welded by many processes among these processes, we can find. Weld techniques that are studied in this report gas tungsten arc welding GTAW and Laser welding. Both are fusion welds.

Laser welding has gained great popularity as a promising joining technology with high quality, high precision, high performance, high speed, good flexibility, and low deformation or distortion, in addition to its many applications due to ease of use with robots, reduced man-power, full automation, systematization, production lines.

Gas tungsten arc welding is the most popular method for welding steels, aluminium and nickel-base alloys. The process provides more precise control of the weld because the arc heat and filler metal are independently controlled.

LPG tanks are typically made of welded steel, aluminium or composites. Steel is by far the most common material, as it is the easiest to fabricate and it is a low-cost material. The LPG tank body is welded by the cylinder body and the head. According to the volumetric size, the cylinder body needs to be divided into several sections, the welding must first weld the inner ring joint.

The objective of this study was the investigation the effect of the welding process on low carbon steel. Two different welding processes (TIG welding and laser welding) were used to joint low carbon steel. To achieve our objective four main techniques of characterization were used which are optical microscopy, scanning electron microscopy, and hardness measurements. This dissertation is divided into four chapters:

- Chapter 1: Laser and TIG welding process.
- Chapter 2: steels and LPG storage tank.
- Chapter 3: Materials and Experimental Procedure.
- Chapter 4: Results and Discussion.

CHAPTER I
LASER AND TIG WELDING PROCESS

I.1 Overview about welding

Welding is a process of connecting metal rods using heat energy either with or without filler metal. Welding is one of the most important joining technologies in manufacture industry. This is due to the welding is one of metal connecting techniques that is easy to implement. The welding has been widely used in the construction of ship, bridges, steel frame, pressure vessel, rail, pipeline and so forth [1].

As metallurgical joining process. the welding process can be divided into three types:

- Solid-state welding.
- Brazing/soldering.
- Fusion welding.

Today, according to applications, each welding technology has its own role in manufacturing. For example, adhesive bonding is used to seal materials in the very low temperature process (< 100 °C); soldering and brazing are generally used in electronic applications; resistance welding is broadly employed for welding nuts and bolts; tungsten inert gas welding is usually applied for architectural fabrications [2].

I.2 Fusion welding

In fusion welding, parts are joined by melting and subsequent solidification of adjacent areas of two parts. Welding may be performed with or without the addition of a filler metal. Depending on the thickness of the part, the weld may consist of one or more individual beads formed by each pass of the heat source along the joint. Fusion welding processes are classified according to the nature of the heat source. An electric arc is used in gas metal arc welding (GMAW) (Fig I-1), gas-tungsten arc welding (GTAW), and submerged arc welding (SAW)(Fig I-2). In laser and electron-beam welding, very high-energy-density beams are used as an energy source. Resistive heating is utilized in the electroslag welding process [3].

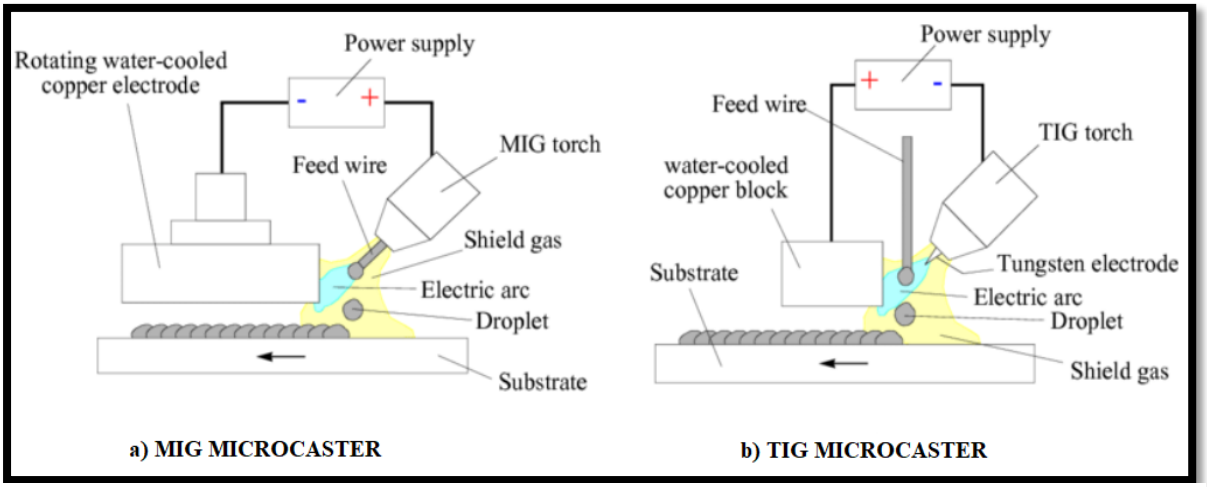

Figure I-1. MIG and TIG Micro caster with water-cooled Copper Electrode [4].

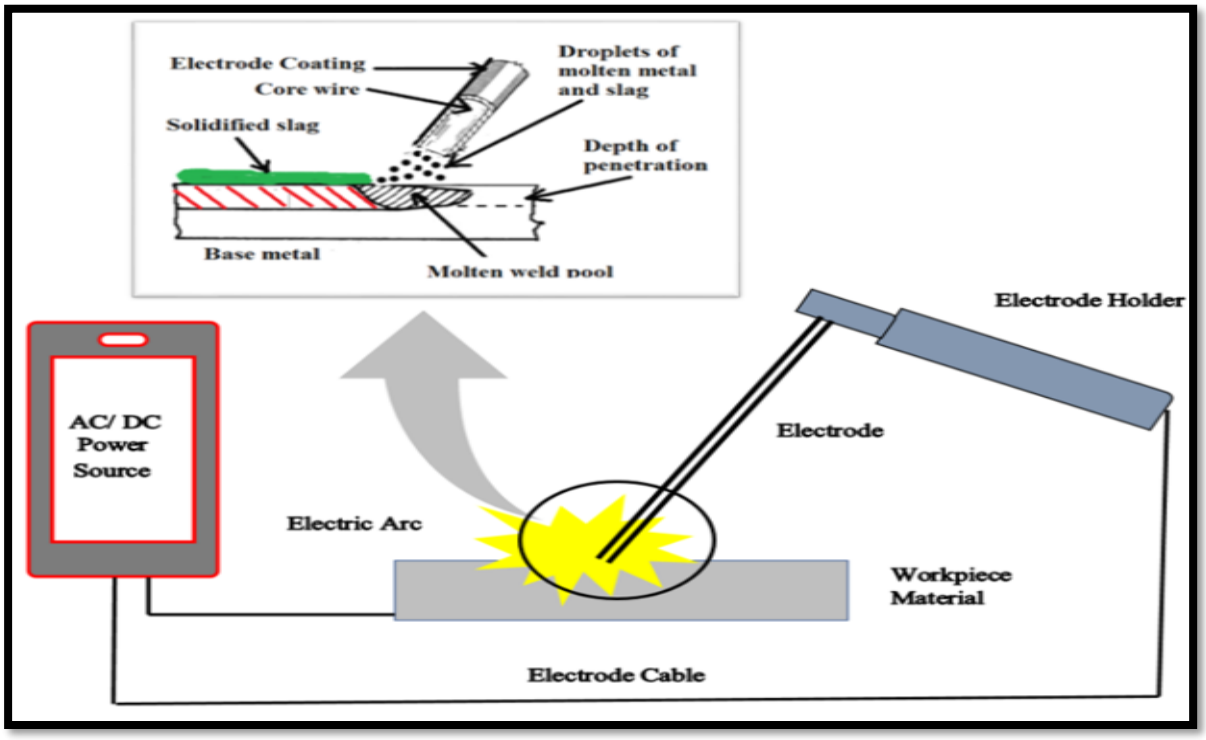

Figure I-2. Input and output inventory for the SMAW process [5].

I.3 Regions of a fusion Weld

Examination of a welded joint reveals distinct micro-structural regions. The fusion zone is associated with melting. The HAZ, though not melted, is affected by the heat from the joining process.

Beyond the HAZ is the unaffected base metal. The fusion zone and HAZ can be further subdivided (Fig I-1) [6].

The fusion zone is described as such because it is the region where melting and solidification occur to form the joint, or weld. Since all metals are crystalline in nature, many possessing cubic crystal lattices, there are general solidification phenomena common to all metals. in many materials, solidification behaviour is very sensitive to composition. For example, the addition of small amounts of carbon and nitrogen to some steels can change their solidification behaviour from ferritic (bcc) to austenitic (fcc). Minute additions of sulphur to steels can promote severe solidification cracking in the fusion zone [6].

The microstructure and properties of the HAZ are solely controlled by the thermal conditions experienced during welding and post weld heat treatment (PWHT). Steel undergoes a phase transformation, which can result in a HAZ that has a radically different microstructure and properties than either the base metal or the fusion zone [6].

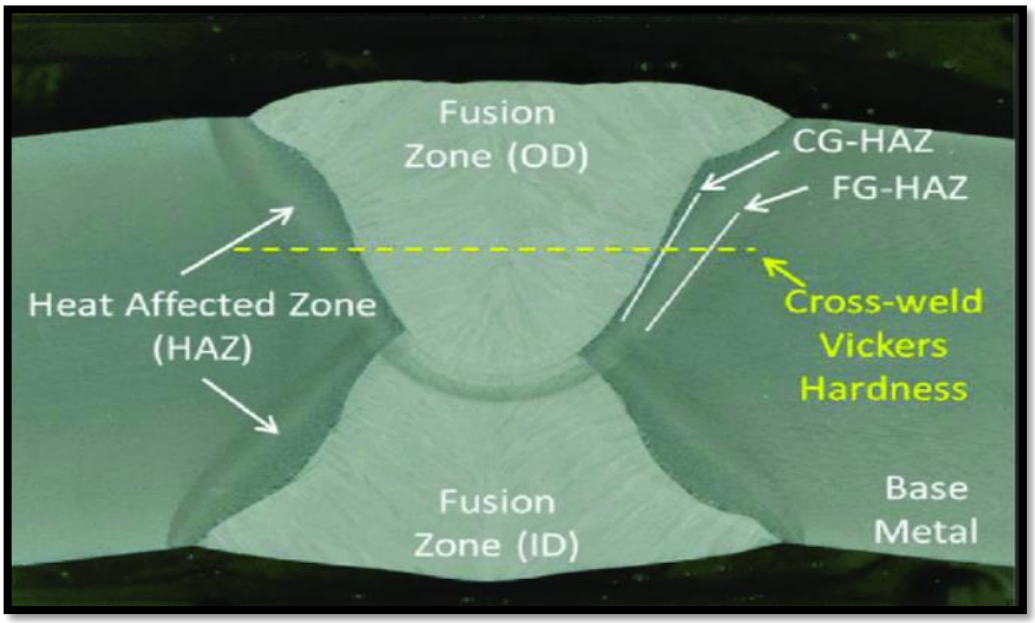

Figure I-1. Constituent zones of a welded joint [7].

The HAZ was subdivided into two regions, the partially melted zone (PMZ) and the “true” heat-affected zone (T-HAZ). The PMZ exists in all fusion welds made in alloys since a transition from 100 % liquid to 100 % solid must occur across the fusion boundary. In addition, other mechanisms were identified that resulted in local melting (or liquation) in a narrow region surrounding the fusion zone. These include grain boundary melting due to segregation and a phenomenon described as

"constitutional liquation" that results from local melting associated with a constituent particle. The designation of a T-HAZ was used to differentiate that region of the HAZ within which all metallurgical reactions occur in the solid state, that is, no melting, or liquation, occurs (Fig I-2) [6].

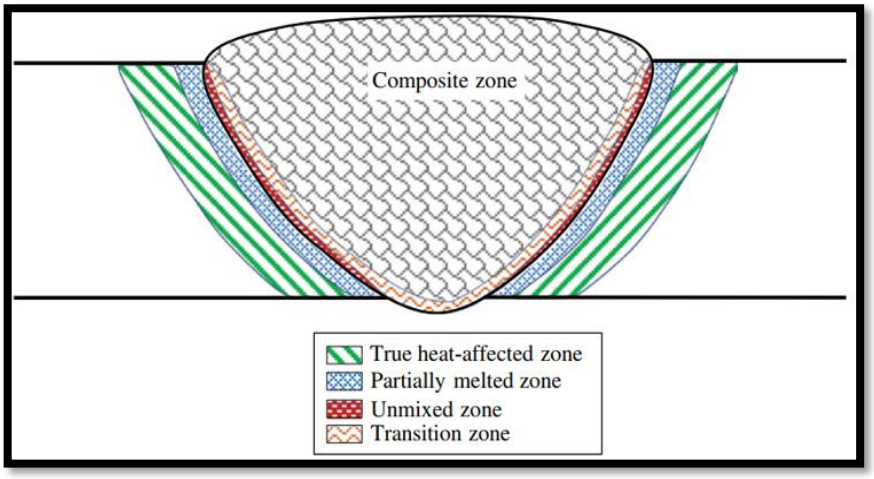

Figure I-2. Modern schematic showing regions of a fusion weld [6].

The slow cooling (air cooling) associated with welding will cause the heat affected zone (HAZ) to experience a wide range of temperatures. Therefore, this range of temperatures is sufficient to anneal part of base metal while the annealing temperature is around 723℃, which makes the heat affected zone divide into subzones (Fig I-3) [8].

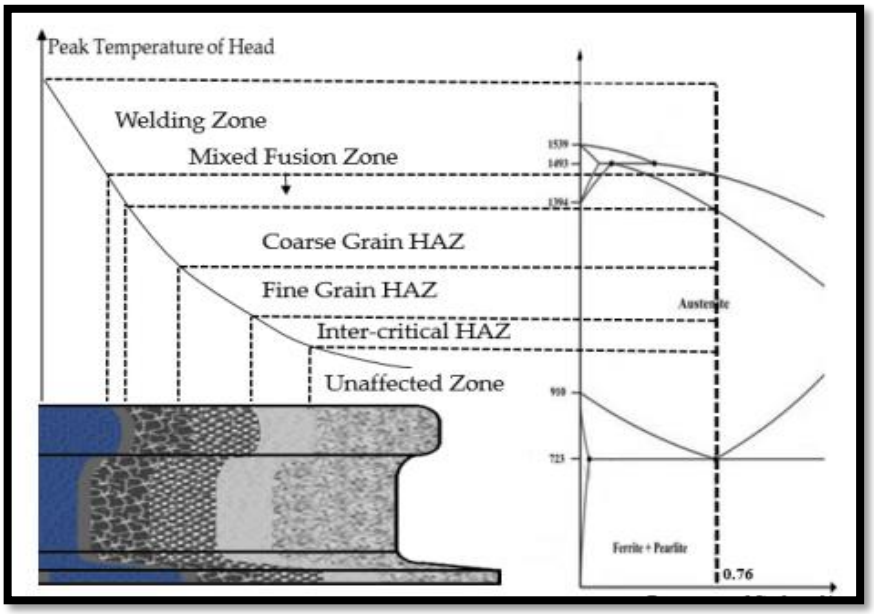

Figure I-3. Constituent zones of a fusion welding combined with iron-carbon phase diagram[8].

I.4 Laser welding

I.4.1 Laser

The word LASER is an acronym, it stands for: (L) Light (A) Amplification (S) Stimulated by the (E) Emission of(R) Radiation, and refers to the way in which the light is generated [3]. All Lasers are optical amplifiers that operate by pumping (exciting) an active medium that is placed between two mirrors, one of which is partially transmitting. The active medium is a collection of specially selected atoms, molecules or ions which can be in a gas, liquid or solid form and which will emit radiation as light waves when excited by the pumping action (Fig I-4) [5].

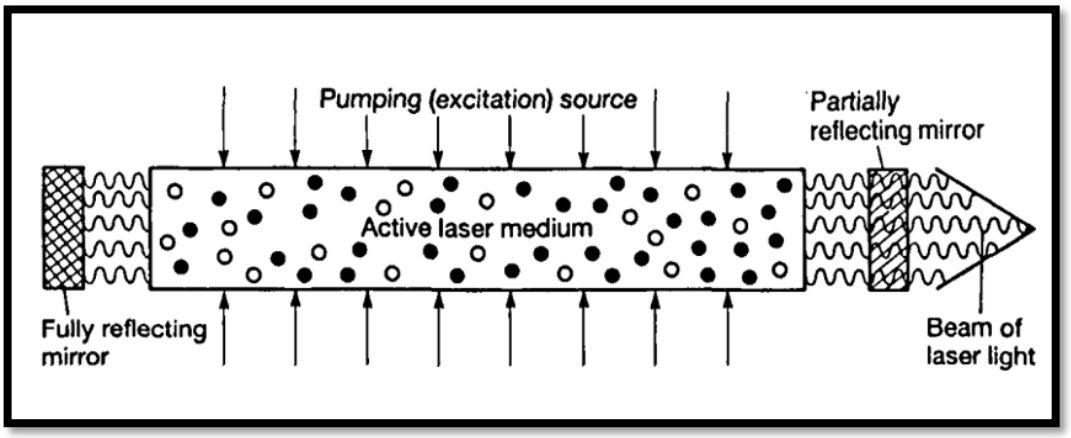

Figure I-4. The basic elements of a laser [5].

I.4.2 Definition of Laser welding

Laser welding is a joining process in which a focused laser beam is coupled to the surface of a material to be welded to generate heat and melt the material [2].

Laser welding is a fusion joining technique used in modern industrial manufacturing processes. The laser welding process has been involved in many manufacturing applications due to an increasing demand of its use in industries. A remarkable aspect of laser welding is an application of highly intensive heat density [W/m^2] which can fabricate a narrow joint weld. In the laser welding process, however, deep penetration modes, e.g., a keyhole and an hour glass, have been found through the change in heat intensity and the welding velocity of a laser beam [9].

I.4.3 Laser welding mechanisms

Laser welding can be carried out by one of two mechanisms:

I.4.4 Conduction limited welding

In this case, the laser acts like a point source of energy moving across the surface of the sheet. Welds performed by this process are roughly semi-circular in cross section. Conduction welding offers an alternative to keyhole welding. Compared with keyhole welding, it is an intrinsically stable process because vaporization phenomena are minimal. However, as with keyhole welding, an on-line process-monitoring system is advantageous for quality assurance to maintain the required penetration depth, which in conduction welding is more sensitive to changes in heat sinking. The maximum penetration is obtained when the surface temperature is just below the boiling point, and so we normally wish to maintain the temperature at this level [10].

I.4.5 Keyhole welding

In this case, the lasers act as a line source of energy penetrating into the body of the material. As the lasers beam is provide the highest power density currently available to the industry (up to 109 W/cm^2) that is focusable on a small spot (down to diameter of 0.1 mm), the absorption of such energy leads to evaporation of the material at the point of contact, forming a cylindrical hole, the keyhole, which may extend through the entire plate thickness in the material. A schematic view of laser keyhole welding is shown in Figure I-5 [11].

Keyhole welding is widely used because it produces welds with high aspect ratios and narrow heat affected zones [12].

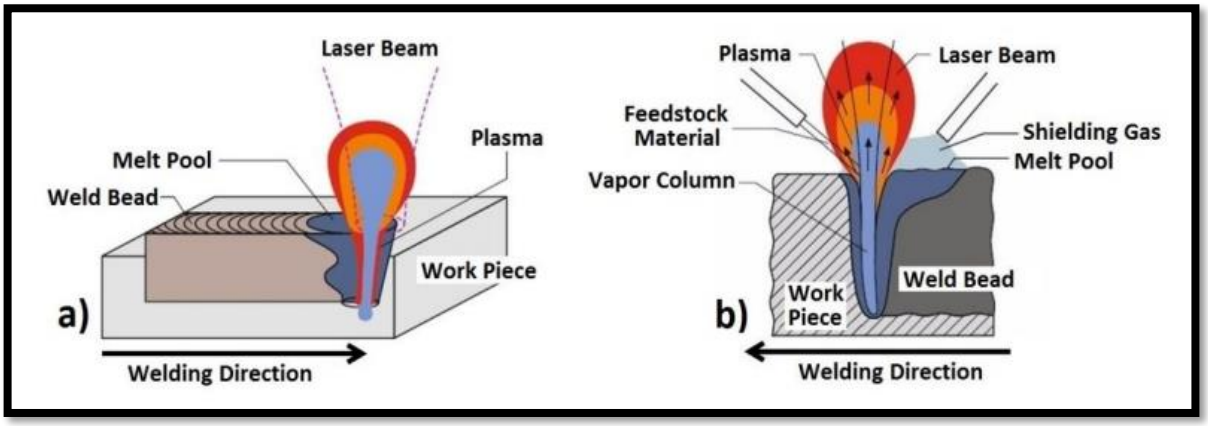

Figure I-5. (a) Autogenous laser keyhole welding and (b) wire feed laser welding schematics[13].

I.4.6 Microstructure of laser beam welds

Although heat input in laser welding is rather low, temperature cycles, and thus recovery and recrystallization in the melt pool and heat, affected zone (HAZ) produces significant microstructure changes. These changes include local variations of grain size, precipitate size, shape, distribution and orientation and, thus, have a strong influence on mechanical properties [14].

The microstructure of the weld is characterized by a narrow heat affected zone, columnar grains and precipitate coarsening in the fusion zone. Texture in the fusion zone is significantly different from the texture of the base material. The residual stress distribution observed is similar at the top and the bottom of the weld, maximum tensile residual stress values are observed in the fusion zone. Tensile tests reveal differences in the mechanical behaviour of the fusion zone and the parent material, which can be related to the differences of texture and the resulting deformation mechanisms [14].

The mechanical properties of the welds are evidently dependent on the microstructural characteristics, and the strengthening in the heat affected zone and fusion zone is mainly attributed to the formation of marten site [15].

Figure I-6.1a presents a macrographic view of welded stainless steel by laser welding process. However, Figure I-6.1b presents the microstructure of this welded stainless steel by laser welding.

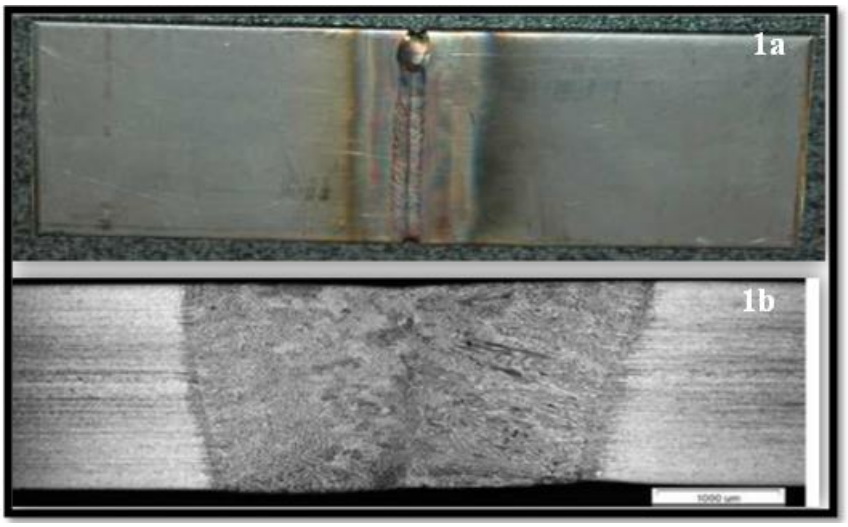

Figure I-6. Macro and microstructure of welded stainless steel by laser welding process [16].

I.4.7 Advantages and applications of laser welding

Laser welding is a well-established joining technology and has been widely applied in the automotive, aerospace, energy, electronic and medical industries. The advantages of laser beam welding include precise energy control, low thermal distortion, small heat affected zones, high welding speed, deep penetration (high weld depth to width ratio) and the elimination of the need for a vacuum chamber. Laser welding is particularly suitable for joining 3D structures, complex assemblies, high precision components and very thin materials including metals, ceramics and polymers. Weld bead geometry is a critical quality factor that can significantly influence the final mechanical properties and microstructures [17].

I.5 Gas Tungsten Arc Welding (GTAW)

I.5.1 Definition of GTA welding

Gas Tungsten Arc welding (GTAW) is an arc welding process that uses an arc between a non-consumable tungsten electrode and the workpiece to establish a weld pool. The process is used with shielding gas and without the application of pressure, and may be used with or without the addition of filler metal [18].

The Gas Tungsten Arc welding (GTAW) process is sometimes referred to as TIG, or heli air. The term TIG is short for Tungsten Inert Gas welding [19].

Because of the high quality of welds that can be produced by gas tungsten arc welding, the process has become an indispensable tool for many manufacturers, including those in the aerospace, nuclear, marine, petrochemical, and semiconductor industries [18].

I.5.2 TIG welding equipment

Four major components make up a GTA welding station. They are (Fig I-7) [20]:

- The welding power supply, often called the welding machine.
- The welding torch, often called a TIG torch.
- The work clamp, sometimes called the ground clamp.
- The shielding gas cylinder.

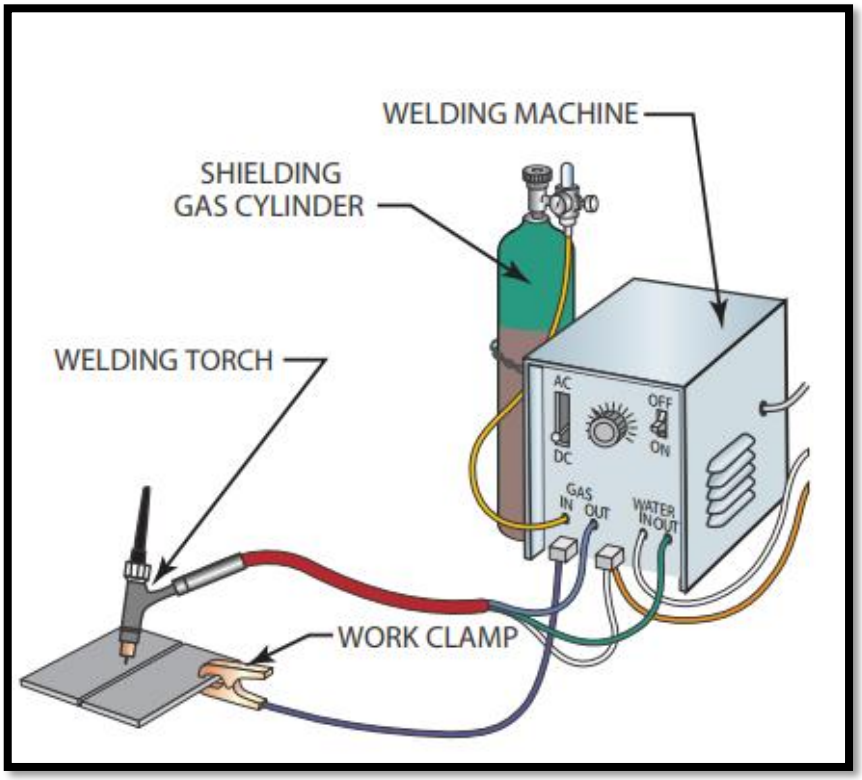

Figure I-7. Tungsten inert gas welding station setup [20].

I.5.3 Basic mechanism of TIG welding

Shielding gas is fed through the torch to provide an inert atmosphere that protects the electrode and the weld pool while the weld metal is solidifying. The electric arc, produced by the passing of current through the conductive ionized shielding gas, is established between the tip of the electrode

and the work piece. The weld starts as heat generated by the arc melts the base metal and establishes a weld pool. The torch is moved along the work piece and the arc progressively melts the surfaces of the joint. If specified, filler metal, usually in the form of wire, is added to the leading edge of the weld pool to fill the joint (Fig I-8) [21].

The filler can be introduced manually or automatically with regarding to types of process. The process itself can be manual, partly mechanized, fully mechanized or automatic. The welding power source delivers direct or alternating current [22].

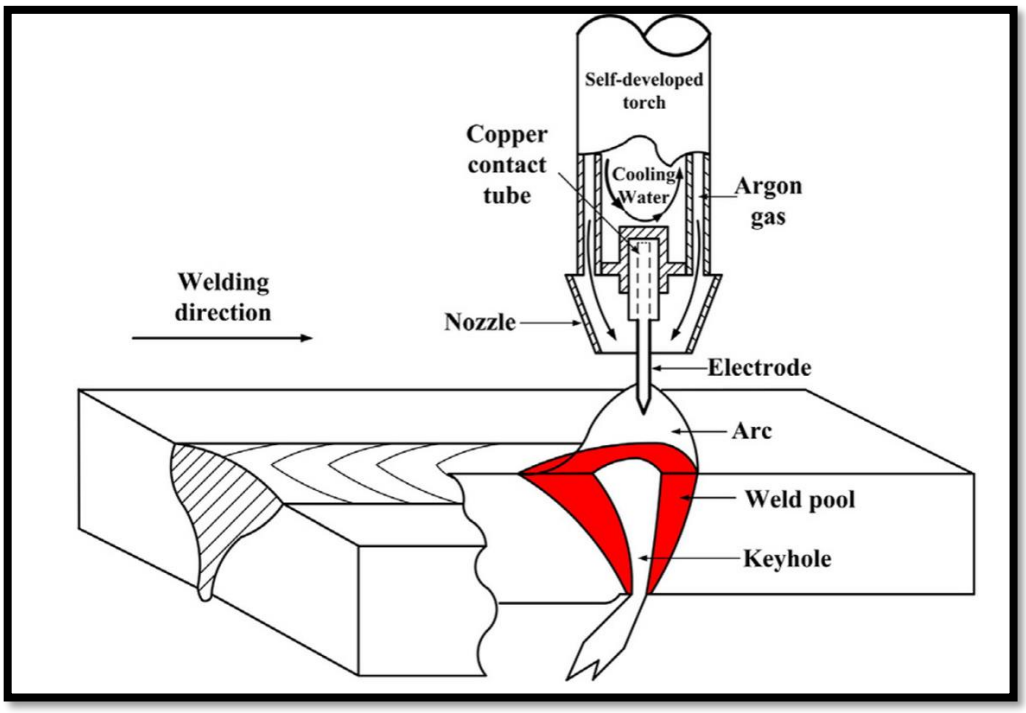

Figure I-8. Gas tungsten arc welding (GTAW) process [21].

I.5.4 Selecting a TIG power source

The TIG power source will be determined by the form and thickness of the welded steel. Recommended items [23]:

- Type of weld able metal (Aluminium, Steel, Stainless, etc.).
- Material thickness to be welded;
- Package solution which suits the application of welding.
- Accessory components which add device value.
- Exercice unit squale, Converter / Inventer – Rectifier.

I.5.5 Advantages of GTAW

Tungsten inert gas (TIG) welding has been applied frequently owing to its advantages such as good protection effect, stable arc, easy adjustment of heat input, less material splash, and nice welding appearance. However, its relatively shallow penetration and low efficiency limit its application [24].

TIG welding is a multi-objective and multi-factor metal fabrication technique. This process can be used for joining a number of common metals such as steel, magnesium and aluminium of thickness 1-6 mm in almost all positions [25].

Gas tungsten arc welding offers advantages for an extensive range of applications, from the high-quality welds required in the aerospace and nuclear industries and the high-speed autogenously welds required in tube and sheet metal manufacturing to the welds typical of fabricating and repair shops, where the ease of operation and the flexibility of the process are welcomed. The process can be automated and is readily programmable to provide precise control of the welding variables with remote welding control capability. Flexibility is gained when using gas tungsten arc welding because the process allows the heat source and filler metal additions to be controlled independently. Excellent control of root pass weld penetration can be maintained.

Welds can be made in any position, and applications are almost unlimited. The process is capable of producing consistent autogenously welds of superior quality at high speeds, spatter-free, and generally with few defects. Almost all metals, including dissimilar metals, can be welded with the GTAW process. A further advantage is that relatively inexpensive power sources can be used [26].

References

[1] Ali, N., Hamza, J. K., & Sofyan, S. E. (2019, May). Effects of welding on the change of microstructure and mechanical properties of low carbon steel. In IOP Conference Series: Materials Science and Engineering (Vol. 523, No. 1, p. 012065). IOP Publishing.

[2] Gong, S., Pang, S., Wang, H., & Zhang, L. (2021). Weld pool dynamics in deep penetration laser welding. Springer Singapore

[3] DebRoy, T., & David, S. A. (1995). Physical processes in fusion welding. Reviews of modern physics, 67(1), 85.

[4] Merz, R., Prinz, F. B., Ramaswami, K., Terk, M., & Weiss, L. E. (1994). Shape deposition manufacturing. In 1994 International Solid Freeform Fabrication Symposium.

[5] Alkahla, I., & Pervaiz, S. (2017, September). Sustainability assessment of shielded metal arc welding (SMAW) process. In IOP conference series: materials science and engineering (Vol. 244, No. 1, p. 012001). IOP Publishing.

[6] Lippold, J. C. (2014). Welding metallurgy and weldability. John Wiley & Sons.

[7] Aucott, L., Wen, S. W., & Dong, H. (2015). The role of Ti carbonitride precipitates on fusion zone strength-toughness in submerged arc welded linepipe joints. Materials Science and Engineering: A, 622, 194-203..

[8] Liu, Y., Tsakadze, Z., Hoh, H. J., Pang, J. H. L., Christian, I., Ng, T. X., & Ng, Y. F. (2018, December). Mechanical properties and microstructural analysis of rail thermite welding joints. In 2018 International Conference on Intelligent Rail Transportation (ICIRT) (pp. 1-4). IEEE.

[9] Koo, B. S. (2013). Simulation of melt penetration and fluid flow behaviour during laser welding. Lehigh University

[10] Bardin, F., Morgan, S., Williams, S., McBride, R., Moore, A. J., Jones, J. D., & Hand, D. P. (2005). Process control of laser conduction welding by thermal imaging measurement with a color camera. Applied optics, 44(32), 6841-6848.

[11] Sokolov, M., &Salminen, A. (2014). Methods for improving laser beam welding efficiency. Physics Procedia, 56, 450-457.

[12] Okon, P., Dearden, G., Watkins, K., Sharp, M., & French, P. (2002, October). Laser welding of aluminium alloy 5083. In International Congress on Applications of Lasers & Electro-Optics (Vol. 2002, No. 1, p. 158364). Laser Institute of America.

[13] Moore, P. L., Howse, D. S., & Wallach, E. R. (2004). Microstructures and properties of laser/arc hybrid welds and autogenous laser welds in pipeline steels. Science and Technology of Welding and Joining, 9(4), 314-322.

[14] Coelho, R. S., Kostka, A., Pinto, H., Riekehr, S., Kocak, M., &Pyzalla, A. R. (2008). Microstructure and mechanical properties of magnesium alloy AZ31B laser beam welds. Materials Science and Engineering: A, 485(1-2), 20-30.

[15] Liu, H., Nakata, K., Yamamoto, N., & Liao, J. (2012). Microstructural characteristics and mechanical properties in laser beam welds of Ti6Al4V alloy. Journal of Materials Science, 47(3), 1460-1470.

[16] A. Kurc-Lisiecka, A. Lisiecki, Laser welding of stainless steel, Journal of Achievements in Materials and Manufacturing Engineering 98/1 (2020) 32-40.

[17] Li, L., Eghlio, R., &Marimuthu, S. (2011). Laser net shapewelding. CIRP annals, 60(1), 223-226.

[18] O'Brien, A. Welding Handbook, Volume 2-Welding Processes, Part 1 . American Welding Society (AWS), 2004. URL https://app. knovel. com/hotlink/toc/id: kpWHVWPP02/welding-handbook-volume/welding-handbook, 699.

[19] Jeffus, L. (2011). Welding and metal fabrication. Cengage Learning.

[20] Jeyaprakash, N., Haile, A., &Arunprasath, M. (2015). The parameters and equipments used in TIG welding: A review. The International Journal of Engineering and Science (IJES), 4(2), 11-20.

[21] Feng, Y., Luo, Z., Liu, Z., Li, Y., Luo, Y., & Huang, Y. (2015). Keyhole gas tungsten arc welding of AISI 316L stainless steel. Materials & Design, 85, 24-31.

[22] Ttulankar, R. W., & Suraj, S. (2013). Dehankar: Automation in Sheet Metal Tig Welding Process. International Journal of Engineering Trends and Technology (IJETT)-Volume4 Issue7-July.

[23] Natrayan, L., Anand, R., & Kumar, S. S. (2021). Optimization of process parameters in TIG welding of AISI 4140 stainless steel using Taguchi technique. Materials Today: Proceedings, 37, 1550-1553.

[24] Wu, H., Chang, Y., Mei, Q., & Liu, D. (2019). Research advances in high-energy TIG arc welding. The International Journal of Advanced Manufacturing Technology, 104(1), 391-410.

[25] Srirangan, A. K., & Paulraj, S. (2016). Multi-response optimization of process parameters for TIG welding of Incoloy 800HT by Taguchi grey relational analysis. Engineering science and technology, an international journal, 19(2), 811-817.

[26] O'Brien, A. Welding Handbook, Volume 2-Welding Processes, Part 1 . American Welding Society (AWS), 2004. URL https://app. knovel. com/hotlink/toc/id: kpWHVWPP02/welding-handbook-volume/welding-handbook, 699.

CHAPTER II
STEELS AND LPG CAR TANK

Introduction

In this chapter, we will see generality about steel, iron carbon equilibrium phase diagram, steel classification and finally an overview about LPG car tank.

II.1 Steel

As a general definition, a steel is an alloy of iron, carbon (under 2% C), and other alloying elements that is capable of being hot and/or cold deformed into various shapes [27].

II.2 Iron carbon equilibrium phase diagram

A study of the constitution and structure of all steels and irons must first start with the iron-carbon equilibrium phase diagram (Fig II-1). It is the foundation on which all heat treatment of steel is based and the basic features of this system influence even the most complex alloy steels [28].

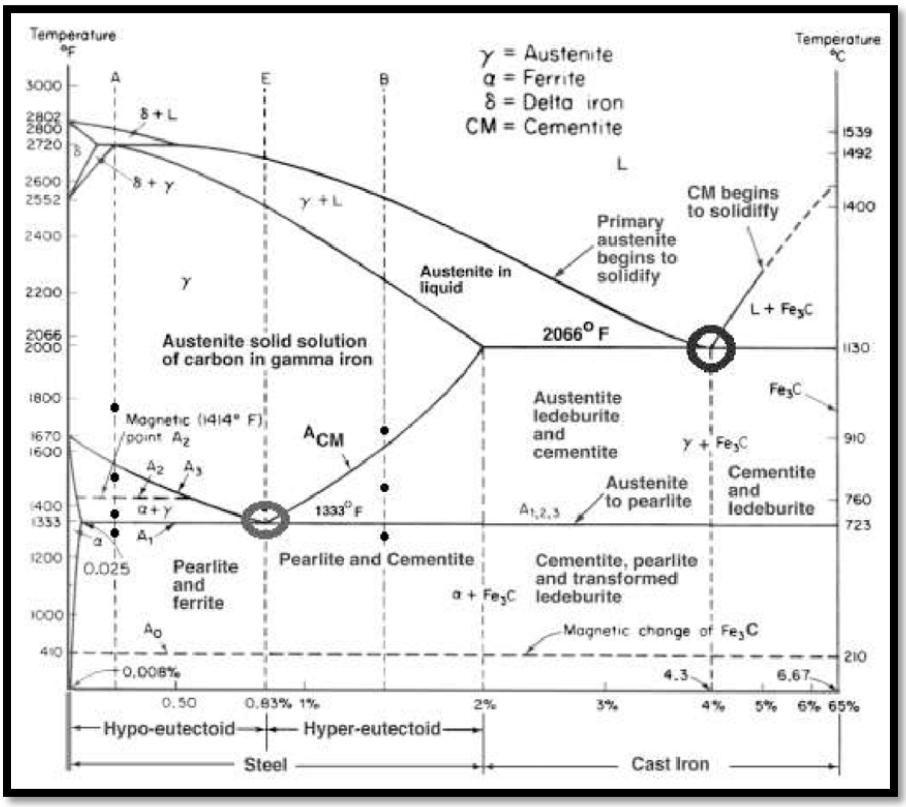

Figure II-1. Iron-Carbon Equilibrium Phase Diagram [29].

According to this diagram, all binary Fe-C alloys containing less than about 2.11wt. % carbon are classified as steels while all those containing higher carbon content are termed cast iron. In addition, it can be noticed that pure iron, at atmospheric pressure, exists in more than one crystal form depending on the temperature. Alpha iron (ferrite) which has the Body Centred Cubic (BCC) structure exists up to 912°C, gamma iron (austenite) which has the Face Centred Cubic (FCC)structure exists between 912° and 1394°C and delta iron (delta ferrite) which has the BCC structure exists from 1394°C to the melting point of pure iron, 1538°C (Fig II-2) [30].

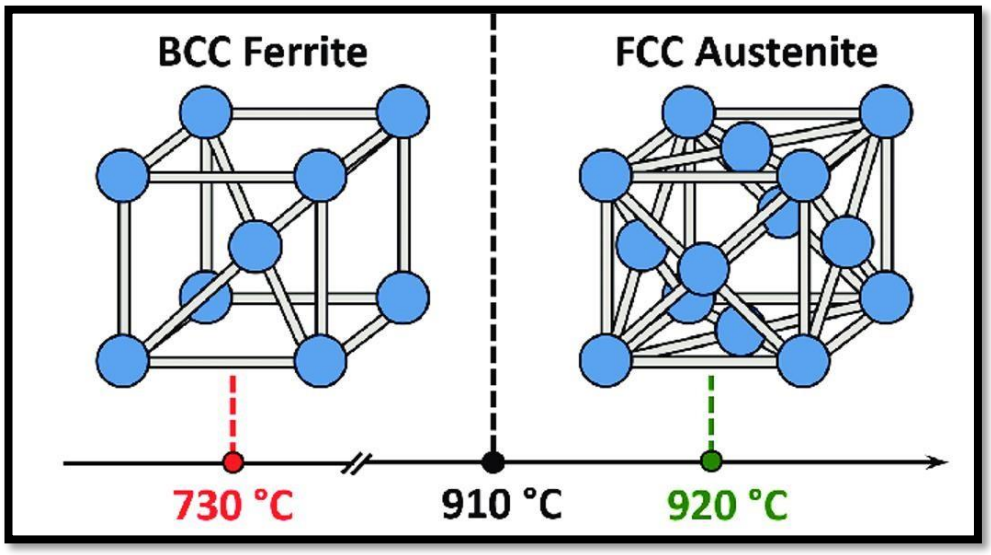

Figure II-2. Lattice structure of two Fe phases regulated by two different temperatures (730 and 920 °C) [31].

There are three critical temperatures which are important in the heat treatment of steel. Firstly, the A1 temperature (723°C) at which the eutectoid reaction occurs. Secondly, the A3 temperature which corresponds to the boundary between the ferrite austenite and austenite fields. This occurs at 910°C for pure iron and it is lowered with the addition of carbon. Finally, the Acme temperature which corresponds to the boundary between cementite-austenite and austenite fields. This temperature increases as the carbon content increases [32].

It is important to notice the great difference in carbon solubility between gamma and alpha iron. During slow cooling of steel containing less than 0.8 wt.% C, ferrite is formed in the range 910-723°C with the rest of austenite becoming enriched in carbon until at 723°C.

The eutectoid reaction. Pearlite is a lamellar mixture of ferrite and iron carbide (cementite) formed via that eutectoid reaction. In the case of high cooling rate, the formation of ferrite and pearlite is suppressed since atomic diffusion is necessary for nucleation and growth of these products. As result, austenite will decompose to non-equilibrium microstructures (Bainite and Marten site) [33].

II.3 Alloy steels

The alloy steels are generally divided into two classes: the low-alloy steels and the high-alloy steels. They are divided according to composition as follows [27]:

type	Alloying elements, %
Low alloy steels	<8
High-alloy steels	>8

Table II-1. Type of alloy steel [27].

II.4 Essential and incidental elements in steel and cast iron

II.4.1 Carbon (C)

An essential alloying element in most steels. Added to increase solid-solution strength and hardness as well as to increase harden ability. Dissolves in iron to form ferrite and austenite. Combines with iron to form a carbide (cementite-Fe3C). The carbide is a component of pearlite [27].

Increasing the carbon content leads to a higher rate of dynamic recrystallization at high temperatures and low strain rates [34].

Carbon stabilized austenite to lower transformation temperatures and that the microstructure became more martensitic in nature. Effects on strength and impact toughness were explainable in terms of a refinement of the microstructure and tempering behavior [35].

II.4.2 Manganese (Mn)

An essential alloying element in most steels. Added to increase solid-solution strength and hardness as well as to increase harden ability. A weak carbide former (greater than iron) [27].

Mn is one of the abundant elements on earth and it is added into steel in order to eliminate noxious sulphur by forming MnS inclusions. Mn in steel stabilizes austenite and it has a higher solubility in austenite than in ferrite [36].

It can impart good corrosion resistance and weld ability or extremely high Strength [36].

II.4.3 Phosphorus(P)

Usually considered an impurity in most steels. Can be added to low-carbon steels to increase strength and hardness. Improves machinability of free-machining steels. Promotes temper embrittlement. Forms an undesirable iron phosphide (Fe3P) at high phosphorus levels (especially in cast irons) [27].

II.4.4 Sulphur (S)

Usually considered an impurity in steel. Added to special steels for improved machinability [27].

II.4.5 Silicon (Si)

An essential alloying element in most steels. Added to increase solid-solution strength and hardness as well as to increase harden ability. Is added to molten steel to remove oxygen (deoxidize). As a result of deoxidation, can form silicate stringers (silicon dioxide inclusions). Does not form a carbide in steels. Improves oxidation resistance. Added to special steels to improve electrical and magnetic properties as well as harden ability. Increases susceptibility to decarburization. Promotes graphitization in cast irons [27].

During steel production up to 0.2 wt.-% silicon is added, primarily to reactwith oxygen. If more than 0.2 wt-% silicon is added, it serves to improve the deep hardening properties [37].

II.4.6 Nickel (Ni)

An essential alloying element in some steels. Added to increase solid-solution strength and hardness as well as to increase harden ability. Toughens steels, especially at low temperatures. Does not form a carbide in steel. Renders high-chromium stainless steels austenitic [27].

Addition of nickel increases the strength of the steel by entering into solid solution in ferrite. It is used in low alloy steels to increase toughness and harden ability. Presence of nickel reduces lattice distortion and cracking during quenching [37].

II.4.7 Aluminum (Al)

An important alloying element in nitride steels and deep-drawing sheet steels. Added to increase strength and hardness of steel by grain-size control (grain refinement). A common deoxidizer. Forms undesirable alumina inclusions (aluminum oxides). A strong nitride former. Does not form a carbide in steel [27].

II.4.8 Titanium (Ti)

An important element in micro alloyed steels. Added to increase strength and hardness of steel by grain-size control (grain refinement). Very strong carbide and nitride former. Important element to tie up nitrogen in steels (protects boron from nitrogen in boron-treated steels). Also, a strong deoxidizer. Can combine with sulphur to form titanium sulphides [27].

Furthermore, the beneficial effects of titanium on the steel properties such as reducing the austenite grain size during rolling, controlling the shape of sulphide inclusions and improving the microstructure and the consequent toughness in the heat-affected zone (HAZ) of weldments have been observed. These benefits have motivated steel makers to add a small amount of titanium to improve the properties of steels, especially for weld ability enhancement. It is well known that a small amount of titanium added to steel will form very stable TiN particles during cooling from solidification [38].

II.4.9 Nitrogen (N)

Added to some micro alloyed steels to increase the amount of nitrides required for strengthening or grain-size control (e.g.in a vanadium steel) [27].

II.5 Plain Carbon Steels

II.5.1 Classification according the composition

Carbon steel properties depend mainly on its carbon content which is widely used in engineering practices. It is categorized into low carbon (mild) steel widely used for heavy structural steelwork, medium carbon steel used for shaft, gearing, pressured structures and railway applications and high carbon steel used for production of springs, gear wheels, vices, cutting tools and brackets in which welding plays an essential role in their fabrication processes (Fig II.3) (Tab II-1) [39]:

subclass	Carbon content, %
Low carbon steels	Under 0,2
Medium carbon steels	0,2-0,5
High carbon steels	Above 0,5

Table II-2. Type of steels [27].

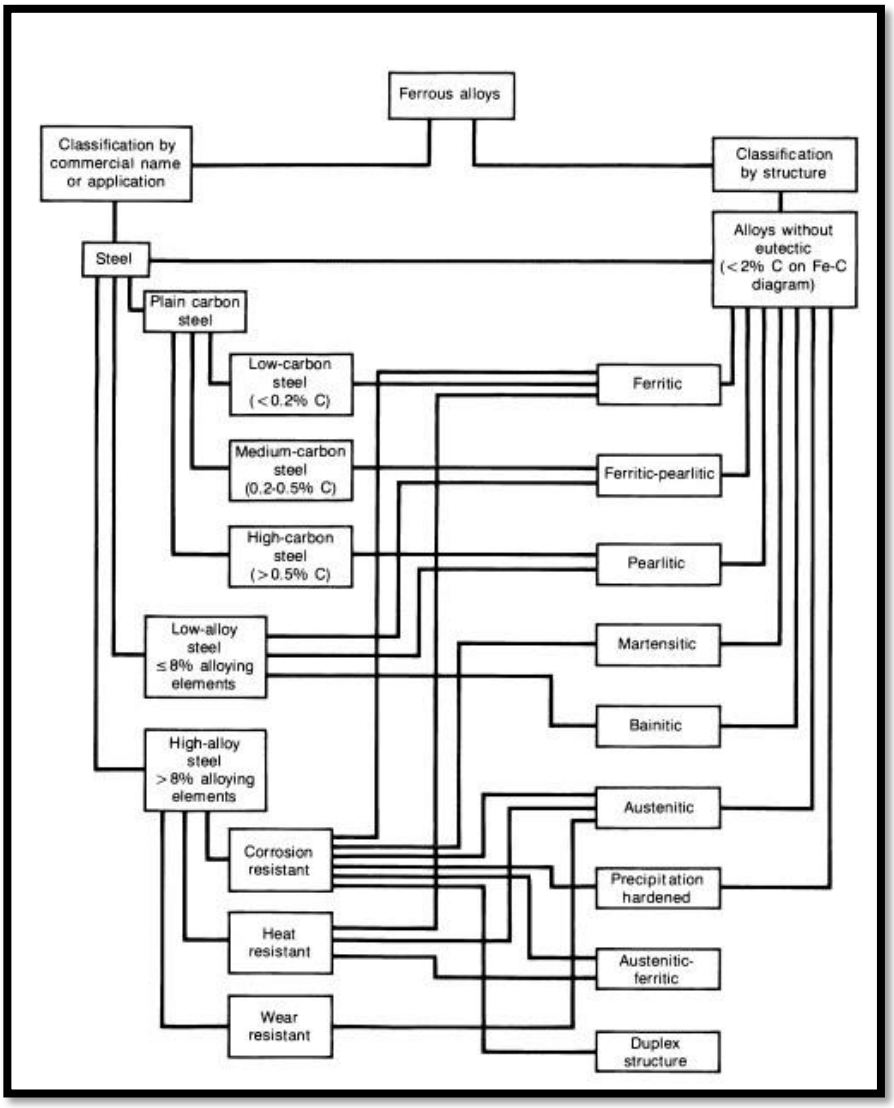

Figure II-3. Classification chart of steels [27].

II.5.2 Low carbon steel

Low Carbon (LC) steels are described as steels that contain less than 0.25% C, with one of the most important products being thin-gauge strip and sheet. The production of these steels with very low carbon and nitrogen contents constitutes the most recent step in the evolution of formable, cold rolled and annealed steels. Low carbon content and additions of elements that have a strong affinity for carbon, such as niobium or titanium; have long been known to promote recrystallisation textures favorable for severe forming operations with a high degree of tolerance to processing variables [40].

- Low carbon steel is classified into two groups:

  A-Dead soft steel (carbon content is 0.03% to 0.08%).

B-Mild steel (Carbon content is 0.08% to 0.2%).

Mild steel is one of the cheap materials among steel and it is very commonly used in all application. It can be easily welded by all common welding technique. It can rust when it comes in contact of oxygen but still it is very hard and durable. It is used where a large quantity of iron is required. It contains a maximum of 0.2% carbon, manganese up to 0.9%along with small amount of phosphorous, sulphur and silicon. Electrical current can easily transfer through it without leaving any effect on the internal structure of the metals. It has Superior welding properties than steel [41].

II.5.3 Microstructure of plain carbon steel

The microstructures of typical low-carbon, medium-carbon, and high-carbon steels are shown in Figure 12,13, and 14, respectively. The low-carbon steel is represented by an AISI/SAE 1010 steel, the medium-carbon steel by an AISI/SAE 1040 steel, and the high-carbon steel by an AISI/SAE 1095 steel [27].

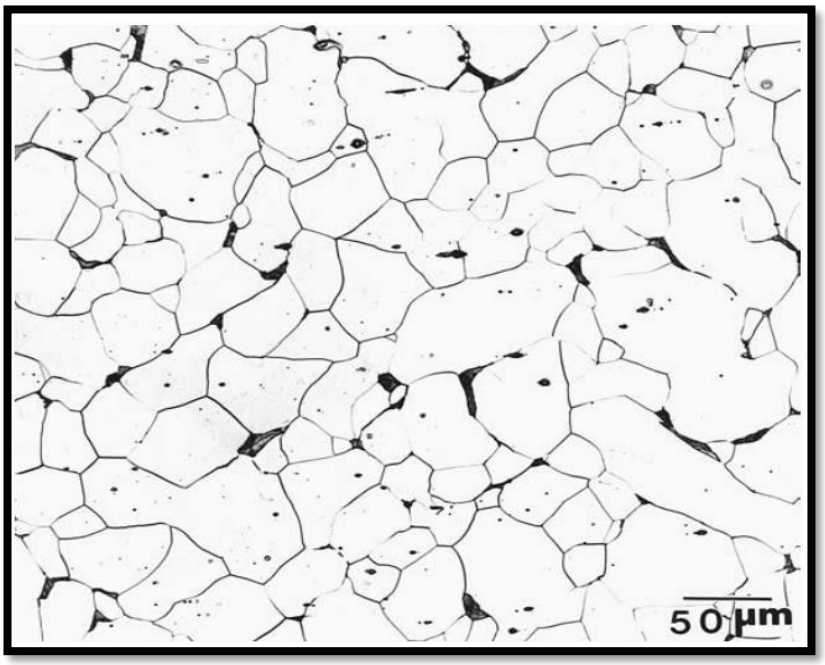

Figure II-4. Micrograph of low-carbon steel showing a matrix of ferrite grains (white etching constituent) and pearlite [27].

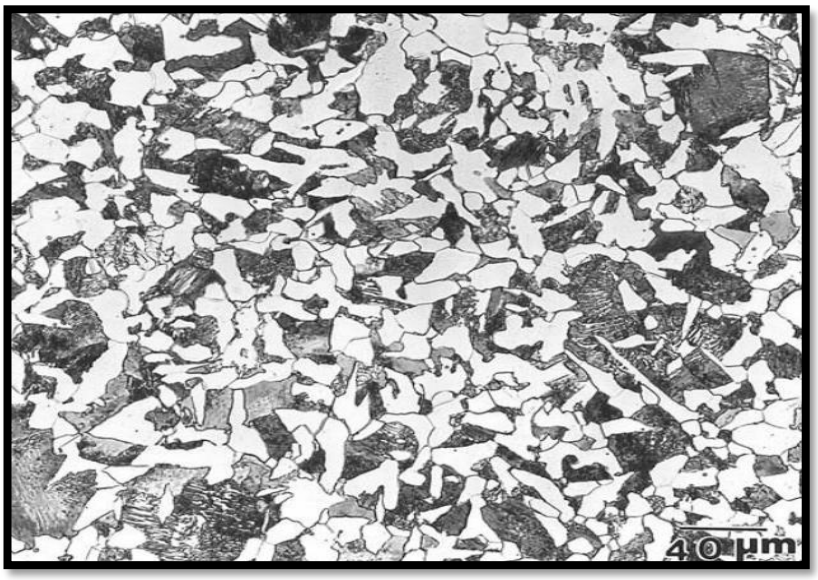

Figure II-5.Micrograph of medium-carbon steel showing ferrite grains (white etching constituent) and pearlite (dark etching constituent) [27].

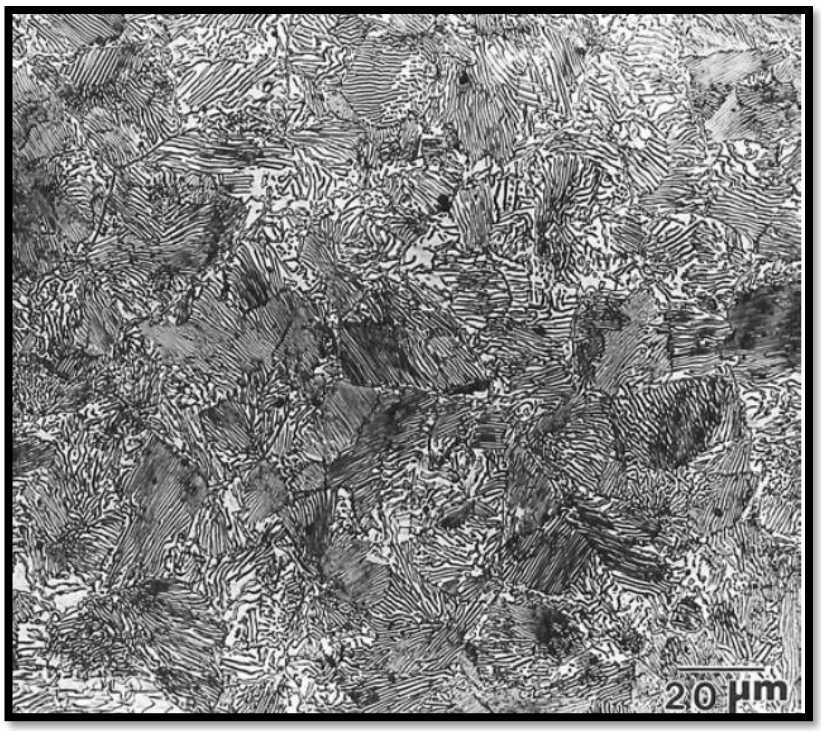

Figure II-6. Micrograph of high-carbon steel showing a matrix of pearlite and some grain-boundary cementite [27].

II.6 Effect of microstructures

The microstructure of steel has a significant effect on the strength of steel. For a steel with a certain composition the microstructure can be altered through varying the processing route used. For example, for strip steels the coiling temperature can be controlled to give varying microstructures in the final coil with varying properties. Changing the amount of second phase in a predominantly ferritic microstructure has a pronounced effect on the strength of the steel. This micro structural change can be achieved through control of composition and processing as mentioned earlier. For structural steels produced as plate and sections with a ferrite + pearlite microstructure relatively small changes in the amount of pearlite and ferrite at low levels (~5-10%) have a relatively small effect on the strength level, especially the yield strength as the surrounding ferrite yields first anyway [41].

II.6.1 Ferritic and pearlitic microstructures

Plain carbon steel is very often used when it consists of a mixture of ferrite and pearlite. The yield and ultimate strengths of these steels are controlled by the mechanical Properties of the ferrite and cementite and micro structural details concerning how they are mixed together. The iron-carbon phase diagram (Figure II-1) shows that, for low carbon steel (between 0.1% and 0.25% carbon), the formation of ferrite starts at about 850^0 C and ends at 723^0 C. It will be remembered that ferrite can contain hardly any carbon. Consequently, the austenite phase transforms to ferrite and cementite (Fe3C). When the cooling rate is slow, the carbon atoms have time to migrate to separate "layers" in the microstructure and to form the structure called pearlite. The ferrite in this mixture is soft and ductile. The cementite constituent is hard and brittle. The mixture (pearlite) has properties between these two extremes. Cementite is a hard and brittle phase. It tends not to deform plastically at ambient temperatures. It can crack. Hence, yield in a pearlitic microstructure is associated with the movement of dislocations in the ferrite. When dislocation sources are activated in the ferrite plates the glide paths of the dislocations are limited by the cementite plates because they cannot slip in the carbide. Instead, they are forced to pile up at or near the ferrite/cementite interfaces. The first consequence of the lamellar microstructure of alternating ductile and hard, brittle plates is an increase in the yield stress of the material compared to that of the ferritic matrix because the inter-lamellar spacing is usually much smaller than the proeutectoid ferrite grain size. We expect that the increase in the yield stress due to the restriction of dislocation glide paths in the ferrite lamellae should be larger the finer the spacing in the pearlite. This expectation turns out to be true. Stress concentrations

are created at the ends of pile ups where the dislocations meet the ferrite carbide interfaces and eventually the carbides can be broken. This occurs more rapidly when the ferrite plates are thicker because more dislocations can participate in an individual pile-up for a given applied stress. The generation of cracks in the cementite plates can initiate general fracture which implies that coarse pearlite should fail before fine pearlite because the cementite plates are expected to crack sooner when the ferrite lamellae are thicker and, also, the cracks will be longer and therefore more able to propagate. This prediction is also true; fine pearlite is both stronger and more ductile than coarse pearlite [42].

Figure II-7 shows the ferrite-pearlite microstructure consisting coarse ferrite and pearlite.

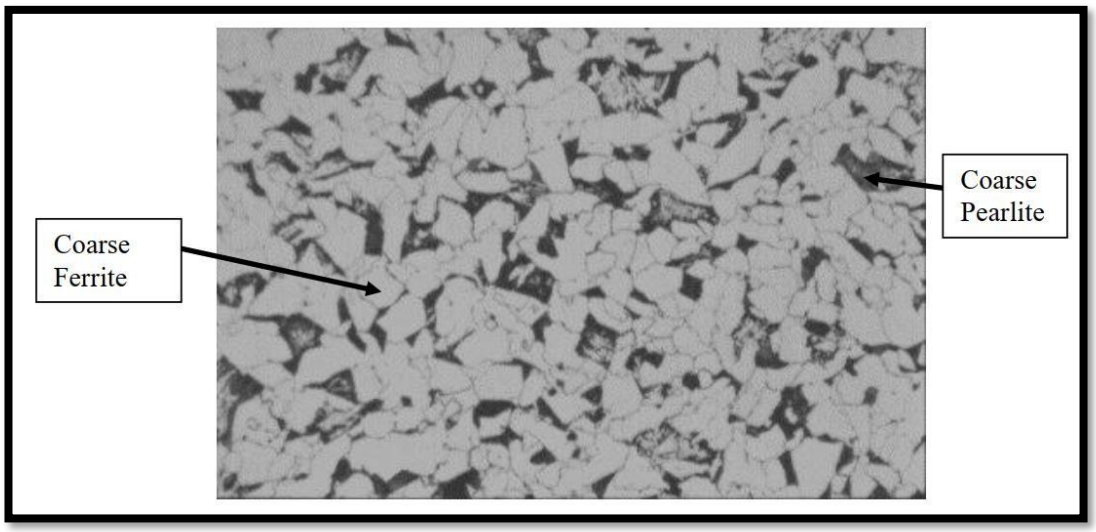

Figure II-7. Coarse ferrite and coarse pearlite steel structure [42].

Ferrite-pearlite microstructure consisting coarse ferrite and pearlite is shown in figure 0-8.

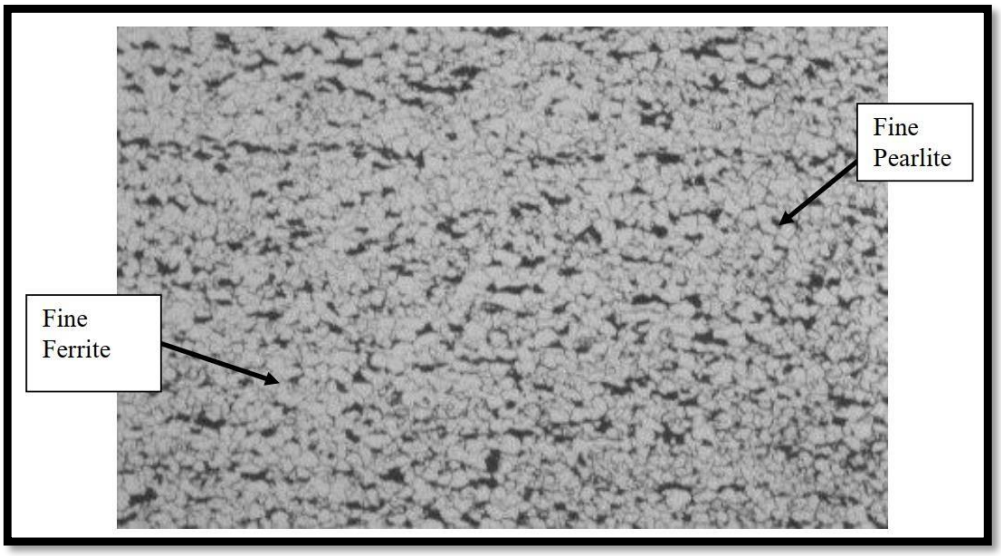

Figure II-8.Fine ferrite and fine pearlite steels microstructure [42].

The cementite network and pearlite microstructure are shown in figure II-9.

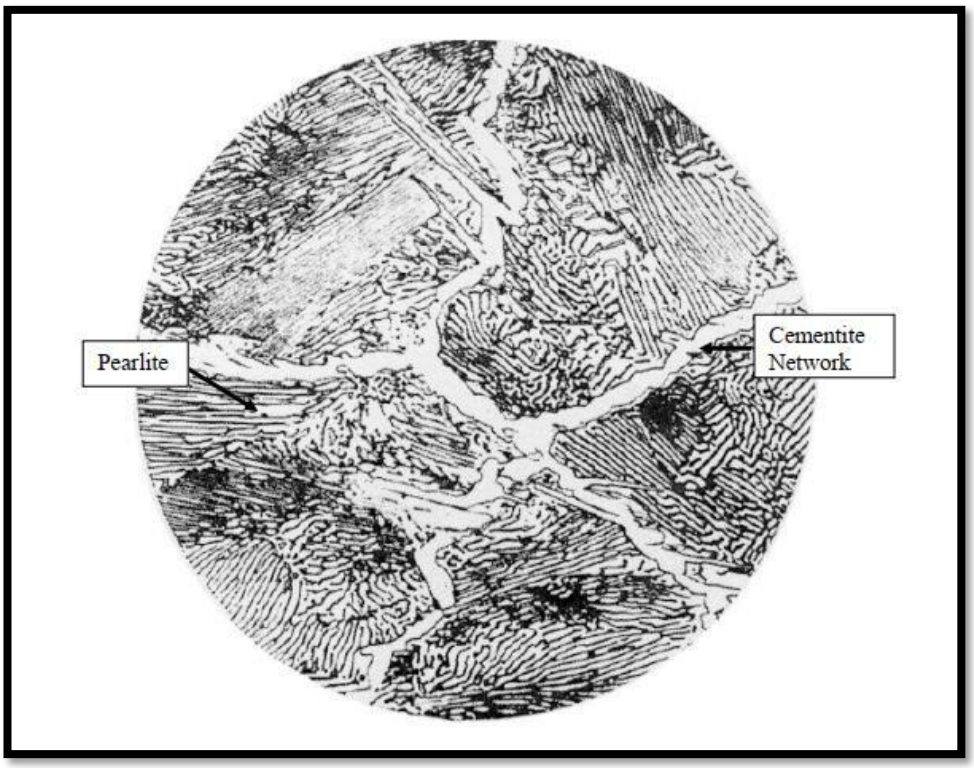

Figure II- 9. Microstructures of cementite and pearlite steels.

II.7 Heat Treatment of Steel

Heat treatment is essentially a process of heating and cooling a material to achieve a desired set of physical and mechanical properties. The properties of materials are dependent upon their structural aspects. The structures may be of different scales of magnitude viz. macrostructure, microstructure, nanostructure, crystal structure, or atomic structure. In general, heat treatment of metals and alloys concerns the change in microstructure. Planned thermal treatment may affect desired changes in the defects structure of metallic crystals; this in turn alters the mechanical properties of the metals and alloys. During the course of heat treatment, the metals and alloys may undergo change in crystal structure (polymorphic transformation), change in chemical composition and change in the degree of order; depending upon the system, these changes may take place either singularly or in combination [43].

II.7.1 Annealing

Annealing is the process of heating the object to single phase field followed by equilibrium cooling to aim at achieving equilibrium microstructures. Depending upon the purpose, various annealing types are carried out at different temperature. A variety of annealing heat treatments are possible. Any annealing process consists of three stages [43]:

- Heating to the desired temperature
- Holding or “soaking” at that temperature
- Slowly cooling, usually to room temperature

II.7.2 Full annealing

Carbon steel is heated to approximately above the upper critical temperature (550-650) °C for 1 hour. Here all the ferrite transforms into austenite. The steel must then cool in the realm of 38 per hour. This results in a coarse pearlite structure. Full annealed steel is soft and ductile with no internal stress [43].

II.7.3 Process annealing

The steel is heated to a temperature below or close to the lower critical temperature (550-650) °C, held at this temperature for some time and then cooled slowly. The purpose is to relive stress in a cold worked carbon steel with less than 0.3%wt c [43].

II.7.4 Recrystallization annealing

Recrystallization annealing is a process of heating cold-worked steel above the recrystallization temperature, holding at that temperature for a predetermined time and then followed by normal air cooling. Recrystallization annealing is carried out for removing strain-hardening effect of multipass cold working operation. In such case, recrystallization annealing is an intermediate process to facilitate further deformation by cold working. On the contrary, recrystallization annealing is also employed as a final heat treatment where removal of cold working effect with replacement by fine equiaxed strain-free grains is derived. Proper selection of time and temperature of annealing enables to achieve fine-grained uniform microstructure comprised of recrystallization [43].

The following observations can be made in any recrystallization process.

1. A minimum amount of deformation is required to effect recrystallization at a particular temperature.
2. Time required to complete recrystallization increases as the temperature of recrystallization is lowered.

3. With increasing deformation percent, the temperature to start recrystallization is decreased.
4. Recrystallized grain size becomes smaller with larger percentage of deformation at a particular temperature.

5. New strain-free grains don’t grow into deformed grains.

6. A metal or alloy with fine initial grain produces smaller recrystallized grain.

II.7.5 Homogenization or diffusion annealing

Homogenization or diffusion annealing is usually carried out for heavy and intricate castings which are prone to significant intercrystalline segregation. Homogenization annealing is carried out to remove the inevitably occurring chemical in homogeneity in heavy alloy steel casting [44].

II.7.6 Normalizing

Normalizing is the heat treatment process, which consists of heating the object to the austenitization temperature, holding it to produce homogeneous austenite and then allowing tube cooled in still air. Normalizing tends to imply a normal cooling of austenite to produce stronger steel

in much shorter time than what can be obtained by full annealing. Due to the fact that normalizing refines the microstructure of the steel thereby improving its toughness, it is quite often employed as the final heat treatment. Normalizing is carried ate temperature 501 C above upper critical temperatures. Being austenitized at higher temperature than annealing, normalizing produces greater homogeneity of austenite but at a lower temperature than homogenizing annealing and in shorter time. Quite often grain size becomes other large after hot working; normalizing of such coarse- grained hot work material gives rise to formation of fine-grained austenite which upon air cooling produces small ferrite grains and fine pearlite in the microstructure of hypoeutectoid steels. This type of microstructures of greater uniformity helps to achieve superior mechanical properties [43].

Low carbon mild steel is quite soft and ductile in the annealed state. Therefore, chips of this ductile material get adhered to the tool tip making the machining quite difficult. Higher becomes the depth of cut, more would be the removal of material and the chances of tool tip jamming with adherent ductile chip will increase. On the contrary, normalizing makes the steel strong and relatively less ductile; this entails the scope of relatively brittle chip formation and chips can easily get away from tool tip. This ultimately improves machinability. Steel compositions may be suitably tailored so that normalized itself can harden the steel or can even alleviate with the conventional hardening and tempering heat treatment, yet achieving equivalent or better mechanicalproperties. For the advantages which can be accrued from normalizing steel the recent efforts to make use of normalizing as the final heat treatment process of new generation steels is noteworthy [43].

II.7.7 Hardening

In case of steels, hardening is possible by quench hardening means; in this case rapid cooling of homogeneous austenite leads to the formation of marten sites as discussed earlier. This marten site is very hard in steel. So, hardening in steel is a typical quench-hardening process. In this process the steel is heated to austenitization temperature; the temperature up to which the steel is to be heated is also decided by whether a homogeneous austenite can be achieved in reasonable period of holding or not [43].

II.8 Steel and low carbon steel in automotive industry

The important factors taking into account by the automotive industry in a manufacturing process of modern cars are: the high ratio of material strength to its density, reduced fuel consumption, safety improvement and limitation of the harmful exhaust gases. It can be achieved by

an optimization of well-known materials and using new groups of materials with the good formability [44].

The growing significance have metallic materials with a high value of strain hardeningexponent and absorbing the large amount of the energy under conditions of high strain rate. The microalloyed structural steels are an example of materials fulfilling requirements of the automotive industry. Their application together with suitable metallurgical technologies enable to manufacture products with the fine-grained structure [44].

A variety of produced vehicles decides about the necessity of manufacturing weld able plates and sheets, characterized by the various tensile strength, formability and work hardening depending on the structure. In the modern automotive industry, the hot-rolled plates of micro alloyed steels are often used. They are manufactured in integrated lines connecting the continuous casting, rolling and accelerated cooling from a finishing rolling temperature. Depending on the specific application and localization of an element in the structure of a vehicle different steels are selected. They are characterized by the various ratio of strength to ductility and ability to energy absorbing during crash events [44].

II.9 Welding of low carbon steel

Low carbon steel is the most common type of steel found in the industry. Welding low carbon steel does not pose any great difficulties to an experienced welder. It is considered an easy task, low carbon steel is the most weld able of all [45].

Boumerzoug et al. [46] studied the effect of arc welding on microstructures and mechanical properties of industrial low carbon steel (0.19 wt. % C). Different zones and some phases are identified. The higher hardness was measured in the FZ (Fig.II-10).

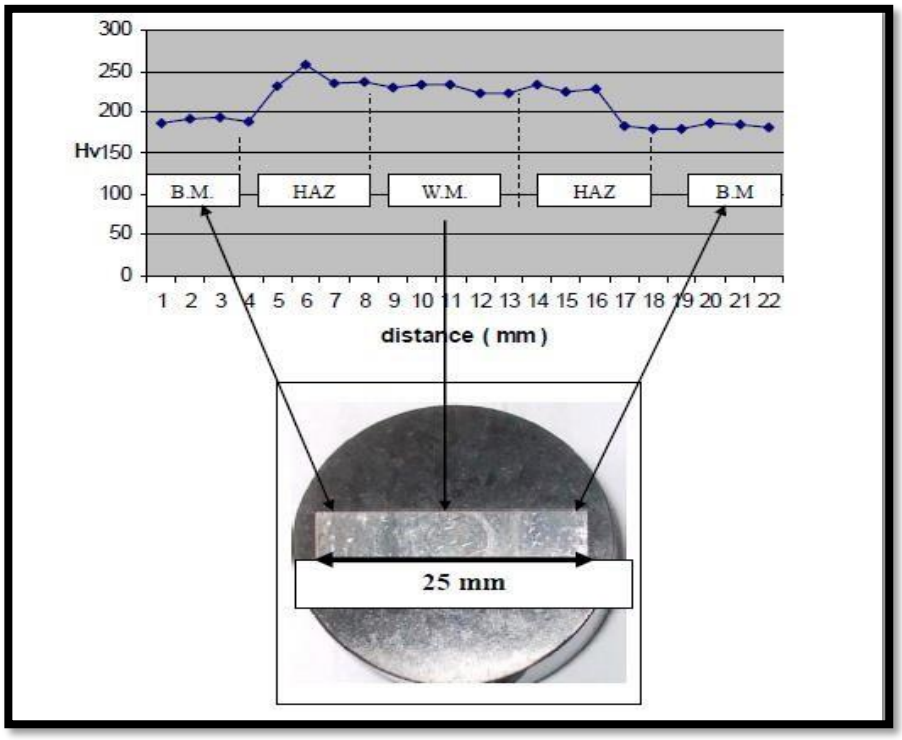

Figure II- 10. Micro hardness measurements on surface S from the base metal across the weld metal after welding of an industrial low carbon steel (0.19 wt.% C) [46].

Ghaini et al. **[47]** investigated the influence of laser pulse energy, duration, and travel speed on weld dimension, microstructure and hardness during overlap laser bead on plate spot welding of low carbon steel. The microstructure resulting from the transformations in the steel material were observed to be quite variable ranging from grain boundary ferrite to Widmansta¨tten ferrite, bainite, and marten site. (Figure II-11).

Figure II-11. Transverse section of A6 sample. Widmansta¨tten ferrite (W) growth from allotriomorphic ferrite (F) grains and marten site (m) plates [47] .

II.10 LPG (Liquefied Petroleum Gas) fuel tanks

The storage fuel tanks, made from aluminum alloys or various types of steel, are used in the automotive industry for safely storing fuel: compressed natural gas (CNG) or liquefied petroleum gas (LPG) [48].

Compression and traction loads applied to the structural design of a storage tank are according to its intended use, size, structure type, materials, and design lifetime, in order to assure product safety and to maintain its essential functions. The pressure cylinders known as LPG fuel tanks and approved by these regulations are commonly used to store the LPG in vehicles. (Fig II-12) [49].

Figure II-12.The types of LPG fuel car tank [49].

The steel used to create storage tanks falls into two main categories: carbon steel and stainless steel. Carbon steel is preferred whenever possible because it is significantly less expensive than stainless. Low-carbon, or mild, steel contains between 0.05% and 0.15% carbon. Because of this, it is quite malleable and can be easily bent, rolled, and welded into desired shapes. This flexible quality makes it easy to form the basic “disc and donut” assemblies that are used to create many finished storage tanks from carbon steel plates [50].

Ryu et al. [51], studied the high heat input electro-gas arc welding of TMCP plate for steel storage tanks. Figure II-13 shows the welded materials. Figure II-14 shows the macrostructure of the welded materials

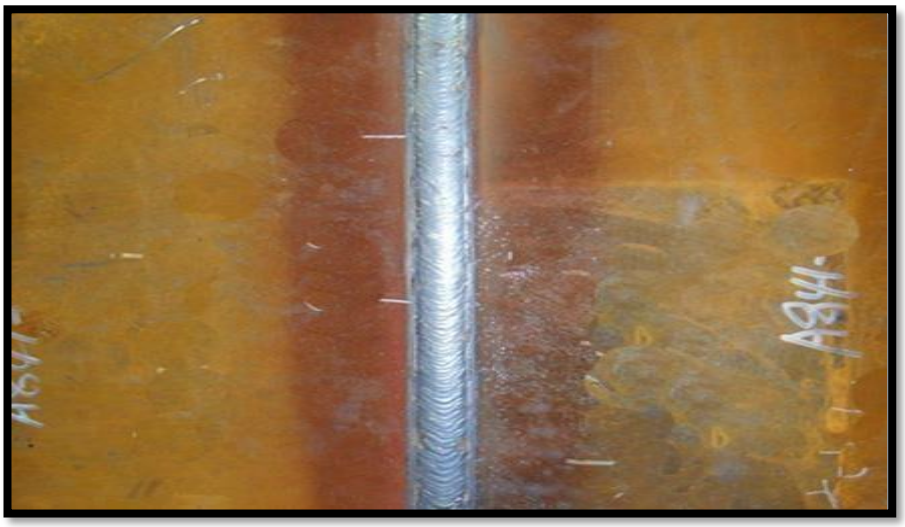

Figure II-13. Microstructure of the welded materials [51].

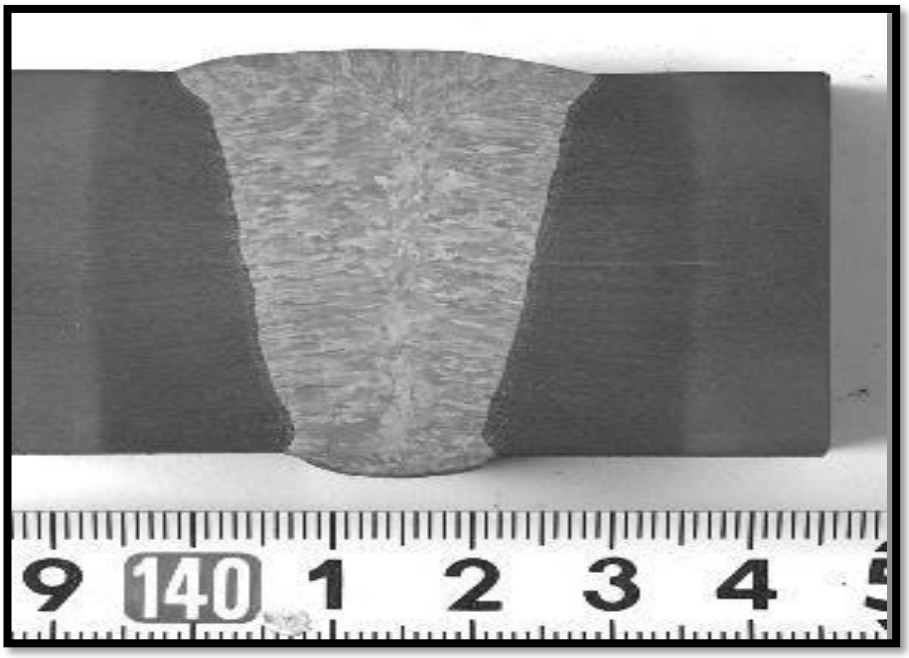

Figure II-14. Macrostructure of the welded materials [51].

Reference

[27] Bramfitt, B. L., &Benscoter, A. O. (2001). Metallographer's guide: practice and procedures for irons and steels. Asm International.

[28] Almojil, M. (2010). Deformation and recrystallisation in low carbon steels. The University of Manchester (United Kingdom).

[29] Callister, W. D., &Rethwisch, D. G. (2018). *Materials science and engineering: an introduction* (Vol. 9). New York: Wiley.

[30] Yamasaki, S., &Bhadeshia, H. K. D. H. (2006). M4C3 precipitation in Fe–C–Mo–V steels and relationship to hydrogen trapping. *Proceedings of the Royal Society A: Mathematical, Physical and Engineering Sciences*, *462*(2072), 2315-2330.

[31] You, Y., Yoshimura, M., Cholake, S., Lee, G. H., Sahajwalla, V., & Joshi, R. (2018). A controlled carburization process to obtain graphene–Fe3C–Fe composites. *Advanced Materials Interfaces*, *5*(16), 1800599.

[32] Almojil, M. (2010). *Deformation and recrystallisation in low carbon steels*. The University of Manchester (United Kingdom).

[33] Krauss, S. E. (2005). Research paradigms and meaning making: A primer. The qualitative report, 10(4), 758-770.

[34] Serajzadeh, S., & Taheri, A. K. (2002). An investigation on the effect of carbon and silicon on flow behavior of steel. Materials & design, 23(3), 271-276.

[35] Keehan, E., Karlsson, L., Andrén, H. O., &Bhadeshia, H. K. D. H. (2006). Influence of carbon, manganese and nickel on microstructure and properties of strong steel weld metals: part 3–increased strength resulting from carbon additions. Science and Technology of Welding and Joining, 11(1), 19-24.

[36] Kim, M. J., & Kim, J. G. (2015). Effect of manganese on the corrosion behavior of low carbon steel in 10 wt.% sulfuric acid. Int. J. Electrochem. Sci, 10, 6872-6885.

[37] Højerslev, C. (2001). Tool steels. Risø National Laboratory.

[38] Wang, S. C. (1991). The effect of titanium and nitrogen contents on the microstructure and mechanical properties of plain carbon steels. Materials Science and Engineering: A, 145(1), 87-94.

[39] Odebiyi, O. S., Adedayo, S. M., Tunji, L. A., &Onuorah, M. O. (2019). A review of weldability of carbon steel in arc-based welding processes. Cogent Engineering, 6(1), 1609180.

[40] Almojil, M. (2010). Deformation and recrystallisation in low carbon steels. The University of Manchester (United Kingdom).

[41] Khamari, B. K., Sahu, P. K., & Biswal, B. B. (2018, June). Microstructure Analysis of Arc Welded Mild Steel Plates. In IOP Conference Series: Materials Science and Engineering (Vol. 377, No. 1, p. 012049). IOP Publishing

[42] MOTALLEB, M. A. (2014). Improvement of mechanical properties of low carbon steel for manufacturing of spindle of jute spinning mill (doctoral dissertation, dhaka university of engineering and technology).

[43] Banerjee, M. K. (2017). 2.1 Fundamentals of heat treating metals and alloys. Comprehensive materials finishing. Elsevier, 1-49.

[44] Singh, M. K. (2016). Application of steel in automotive industry. International Journal of Emerging Technology and Advanced Engineering, 6(7), 246-253.

[45] Ethan Bale, Welding Low Carbon Steel, download on 12/06/2022 from https://mewelding.com/low-carbon-steels/

[46] Zakaria Boumerzoug, Chemseddine Derfouf, Thierry Baudin, Engineering, 2010, 2, 502-506.

[47] F. Malek Ghaini, M.J. Hamedi, M.J. Torkamany and J. Sabbaghzadeh, Weld metal microstructural characteristics in pulsed Nd: YAG laser welding, Scripta Materialia 56 (2007) 955–958.

[48] Ţălu, M., & ŢĂLU, Ș. (2018). Design and Optimization of Pressurized Toroidal LPG Fuel Tanks with Variable Section. *Hidraulica*, (1).

[49] Opriţoiu, P. (2021). Comparative Study of the Effect of the Compression and Traction Loads on the Stress and Deformation of a Toroidal LPG Tank. *Hidraulica*, (2).

[50] Metal Grades for Carbon Steel Tanks and Stainless Steel Storage Tanks, download on 12/06/2022 from https://www.southernmetalfab.com/blog/steel-storage-tanks-metal-grades/

[51] Kang-Mook Ryu, Dae-Woo Kim, Jin-Woo Lee, Hwan-Cheol Bang, High Heat Input Electro-gas Arc Welding of TMCP Plate for Steel Storage Tanks , Journal of Welding and Joining, Vol.35 No.6 (2017) pp. 27-31

CHAPTER III

Materials and Experimental Procedure

Introduction

This chapter presents the base materials used and also the techniques of welding of low carbon steel. In addition, the techniques of characterization are also presented with necessary details.

III.1 Base materials

For the two-welding process (laser and TIG welding), the type of steel used is BS2 low carbon steel which the chemical composition is given in table III-1. The steel was obtained in the form of plates which had a warm rolled. The thickness of welded plats is equal to 3 mm (Fig.III-1)

Figure III-1. Welded plats of low carbon steel by TIG and Laser welding processes.

chemical composition							
C%	MN%	SI%	S%	P%	AL%	TI%	N%
0.15	0.63	0.19	0.007	0.014	0.039	0.012	0.002

Table III- 1. Chemical composition of BS2 steel.

III.2 Mechanical properties of the basic material

The mechanical properties of BS2 low carbon steel that have been used in this study is given in table III-2.

Mechanical properties		
Re **N/mm²**	**Rm** N/mm²	**A%**
378	**461**	**28**

Table III- 2. Mechanical properties

III.3 Welding processes

In this investigation, two welding processes were used: TIG and laser welding.

III.3.1 TIG welding process

The TIG welding was done in the industrial company of metal equipment manufacture for storage of fuels -PETROGEL BATNA**.**

III.3.1.1 Machine of welding

The TIG welding machine is shown in Figure III-2.

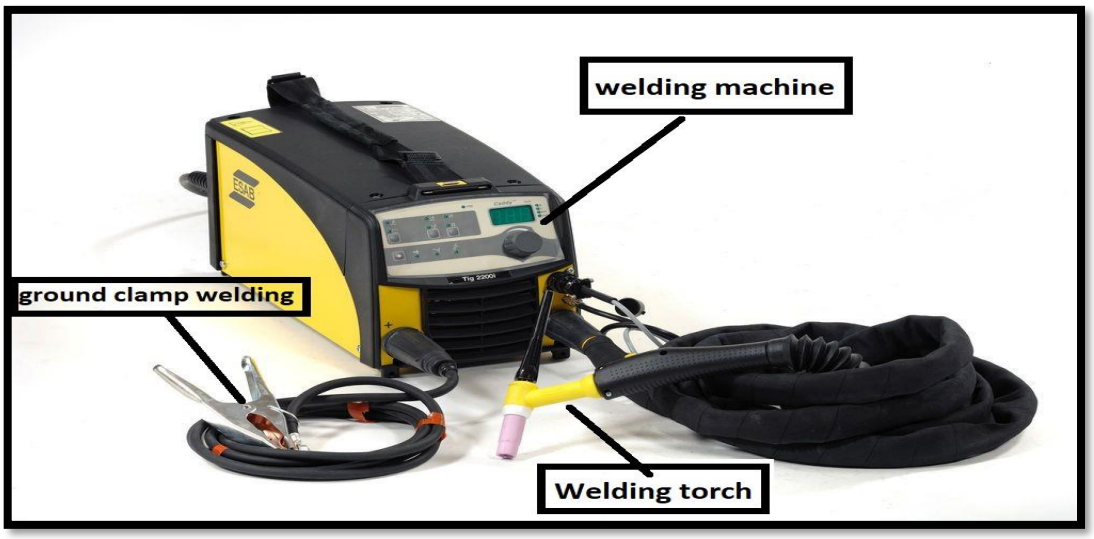

Figure III-2. TIG welding machine (2200i).

III.3.1.2 Characteristics of the TIG welding

The characteristics of the TIG welding process are:

- Homogeneous welding (filler metal is also a carbon steel, same material of the used plats). (Fig.III.3.1.)
- Without chamfer (the thickness of the plats is = 3 mm).
- Under gas protection (The shielding gas is Argan).
- The welding was divided into two steps are:

❖Step 01: **Step of filling**:

- The current intensity = 84 A.
- Filler metal diameter = 2.4 mm.

❖Step 02: **Step of confirmation**

- The current intensity = 97 A.
- Filler metal diameter = 3 mm.

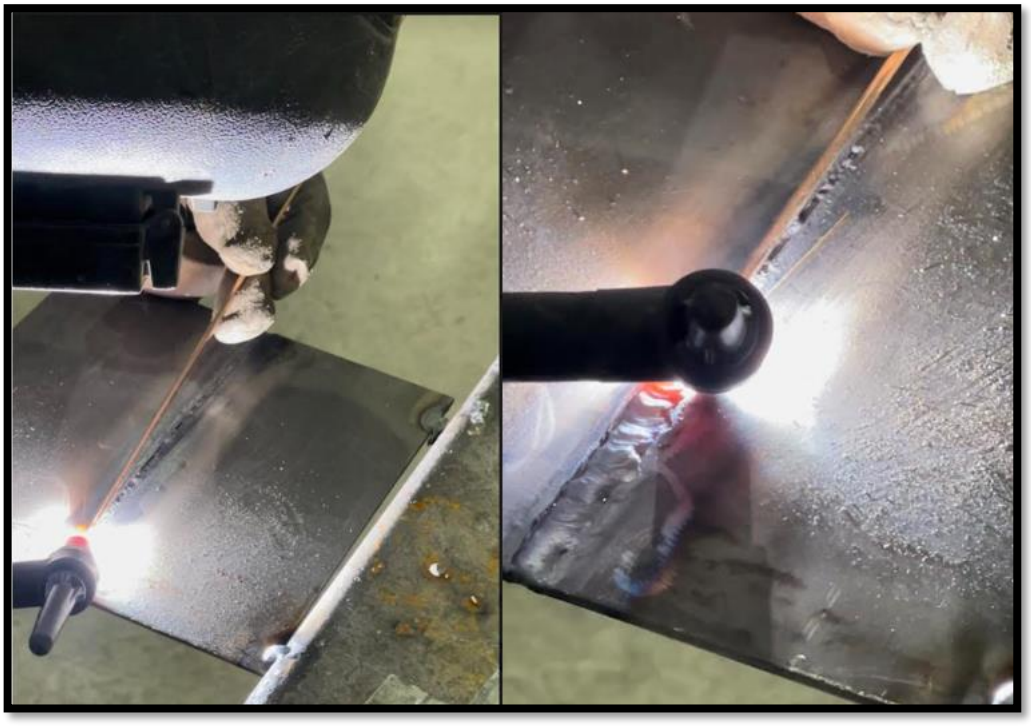

Figure III-3. TIG welding of the plats.

III.3.1.3 Parameters of the TIG welding process

The parameters of this process were presented in table III-3:

TIG welding parameters	Units	Levels		Figure
		filling	confirmation	
current (A)	A	84	97	
filler rod	mm	2.4	3	
gaz sheild pression (Argon)	bar	18		
tungsten electrode	mm	2.4		
thickness of plats	mm	3		
joint	mm	1		

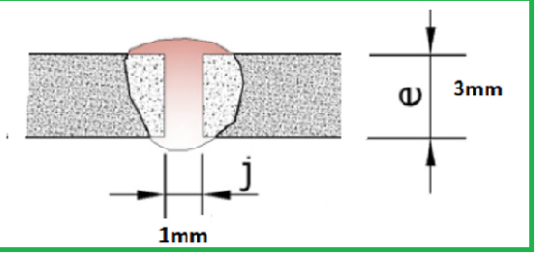

Table III-3. Parameters of TIG welding.

III.3.2 Laser welding process

Two plates of BS2 low carbon steel were welded by a laser beam. The focus point of the laser was in the middle of the joining line of the two pieces as presented in Figure III-4 and shown in Figure III-5.

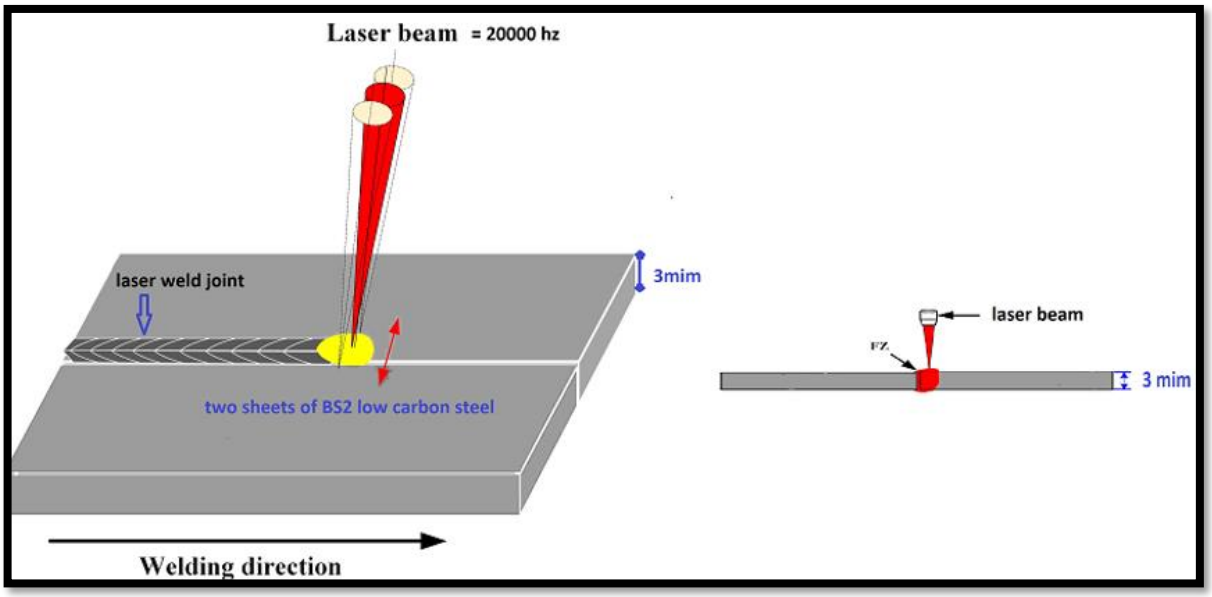

Figure III-4. Schema of Laser welding process.

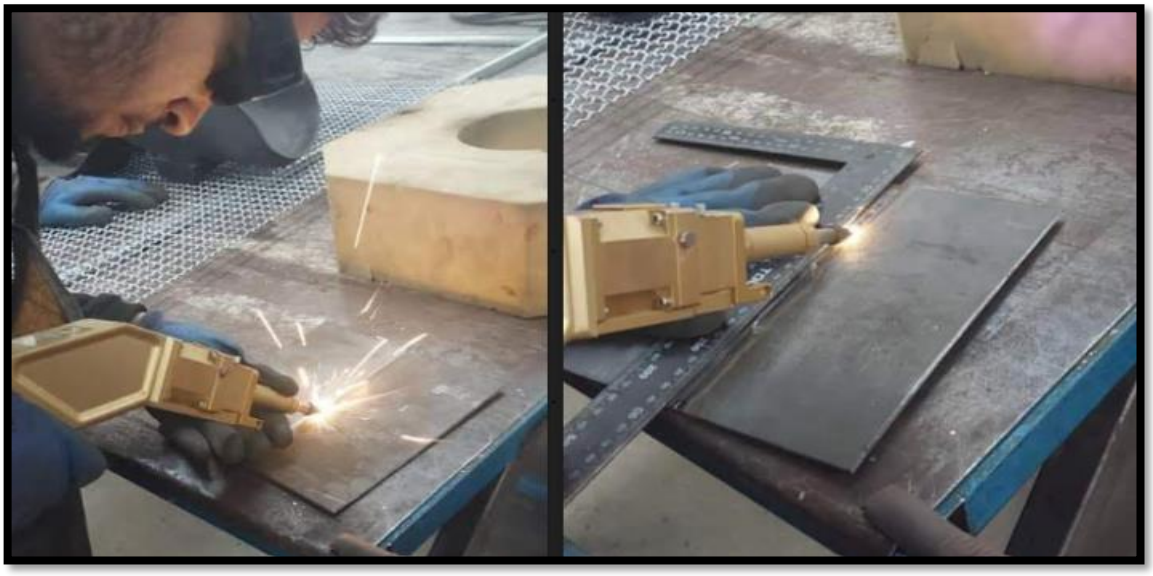

Figure III-5. Laser welding process.

III.3.2.1 Machine of welding

The laser welding machine is a handle fiber laser machine as presented in figure III-6.

Figure III-6. Machine of Laser welding.

III.3.2.2 Parameters of the Laser welding process

Laser welding Parameters		Figure
Laser power	2 KW	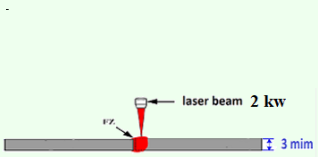
Laser mode	Welding	
Move mode	Continuous	
Impulse frequency	20000 HZ	
Shield gas	Argon	
Shield gas pression	20 l/min	
Thickness of plats	3 mm	
Join	1 mm	

Table III-4. Parameters of Laser welding.

III.4 Metallographic preparation of samples

We noticed that to reveal the microstructure of the deposit and the substrate, a metallographic preparation was performed in the samples.

III.4.1 Cutting and mounting

All samples were cutted by a manual saw under water then they have a cold mounting in epoxy resins (air hardening in plastic molds).

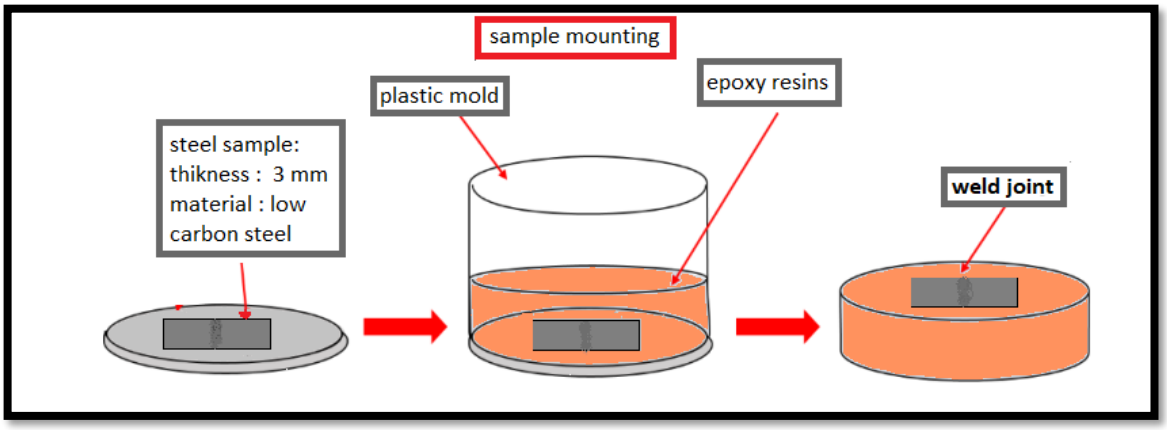

Figure III-7. Steps of the mounting of sample.

III.4.2 Polishing

The coated samples are mechanically polished on mechanical polisher (The type of machine is MECAPOL) (Fig.III-9) by abrasive papers with different grain sizes from 120 to 1200, followed by a felted fabric with the addition of lubricant and diamond paste. After each polishing, the samples are cleaned with distilled water and finally dried.

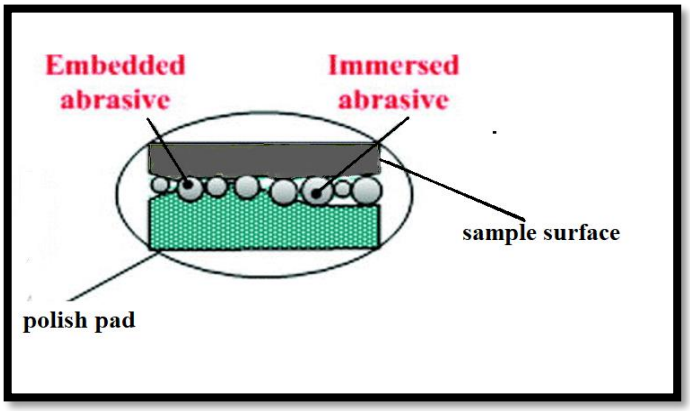

Figure III-8. Interaction between the samples surface and grain of polish pad during the mechanical polishing.

Figure III-9. Polishing machine MECAPOL.

III.4.3 Chemical etching

The samples are chemically etched by a reagent called Nital (Nitric acid + Ethanol), with 2% Nital (Fig III-10):

- Ethanol C_2H_6O = 98 % - Nitric acid HNO_3 = 2%.
- Etching time = 40 sec.

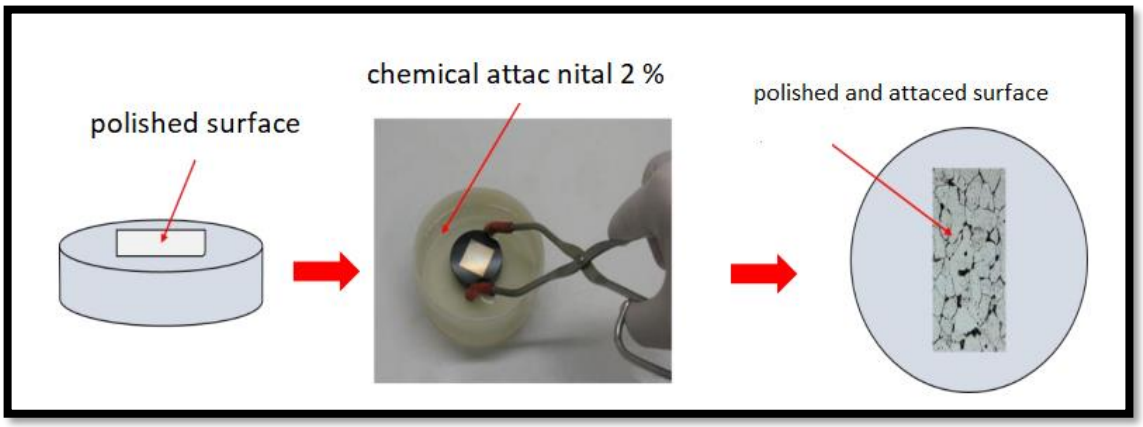

Figure III- 10. Chemical etching process.

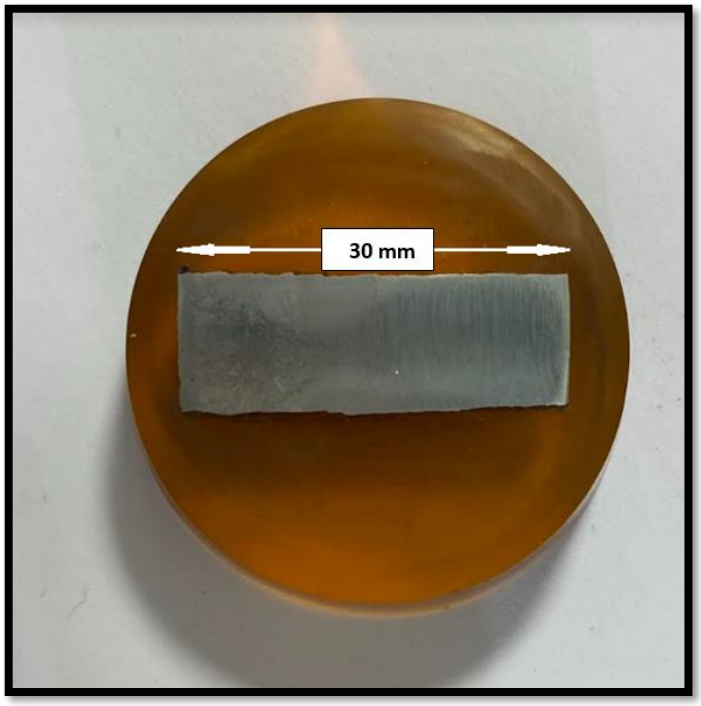

Figure III-11 .TIG sample after metallographic preparation.

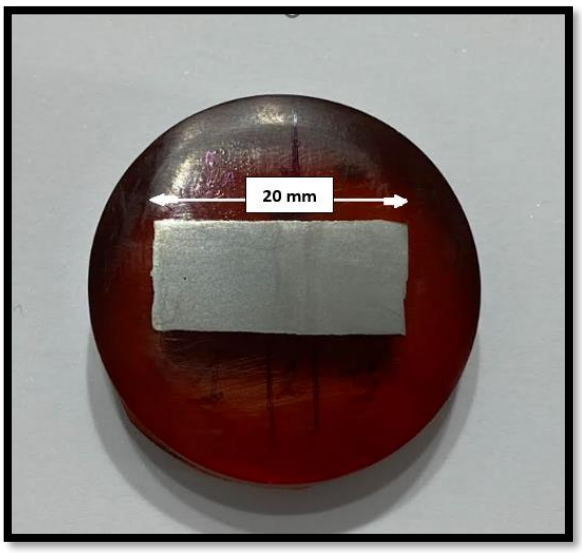

Figure III-12. Laser sample after metallographic preparation.

III.5 Techniques of characterization

To achieve our objective, the main techniques used in this study are optical microscopy and hardness measurements.

III.5.1 Optical observations

The optical observations were conducted by using an optical microscope with different magnifications. The type of the optical microscope is Olympus (Fig III-13).

Figure III- 13. Optical microscope (Type Olympus).

III.5.2 X-ray diffraction

X ray diffraction (XRD) is a main technique for the phase identification of materials based on information from unit cell dimensions. The obtained pattern from XRD helps to identify the various crystalline phases and to study their internal structural properties thoroughly. An XRD pattern reveals information about the various phases present in the crystalline composition under study and also gives information about particle/crystal size, crystallinity of the sample, solid solution, stress, and texture. The Bragg's law explains the relationship between an x- ray light shooting into and its reflection off from crystal surface[52].

Bragg's Law as follows:

$$n\lambda = 2d\sin\Theta$$

Where n is the diffraction order, λ is the wavelength of the incident X-ray beam source, $d$is the diffraction interplanar distance and θ is the diffraction angle. A schematic illustration of Bragg's condition is presented in Figure III-14. Analysis of the phases was conducted using X-ray diffractometer, Siemens model (BRUKER D8 DISCOVER) with Cu Kα radiation, in 2θ range from 10° to 90°. The results were analyzed by using Expert high score plus software and presented by origin 8. Figure III-15 shows X-ray diffractometer used in this research work.

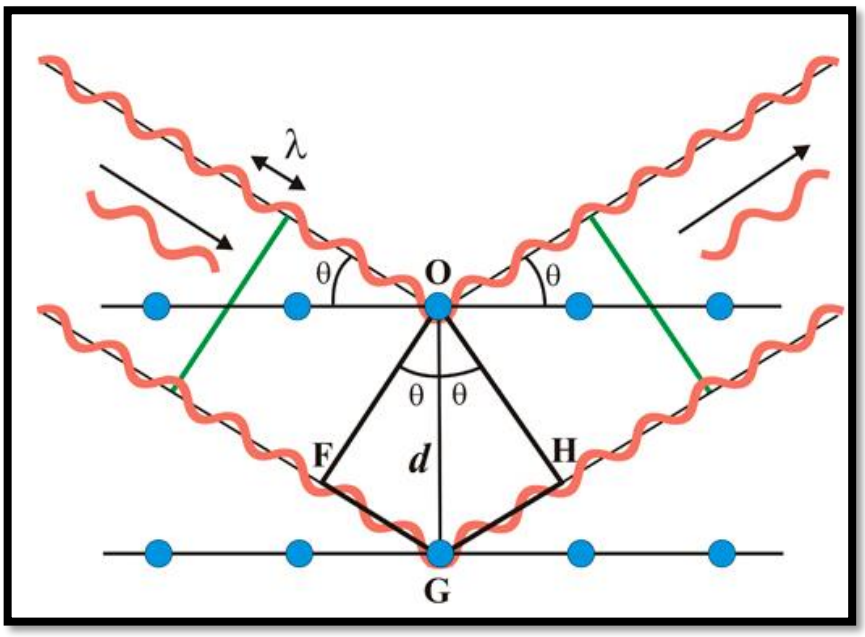

Figure III-14.Schematic illustration of Bragg's condition [52].

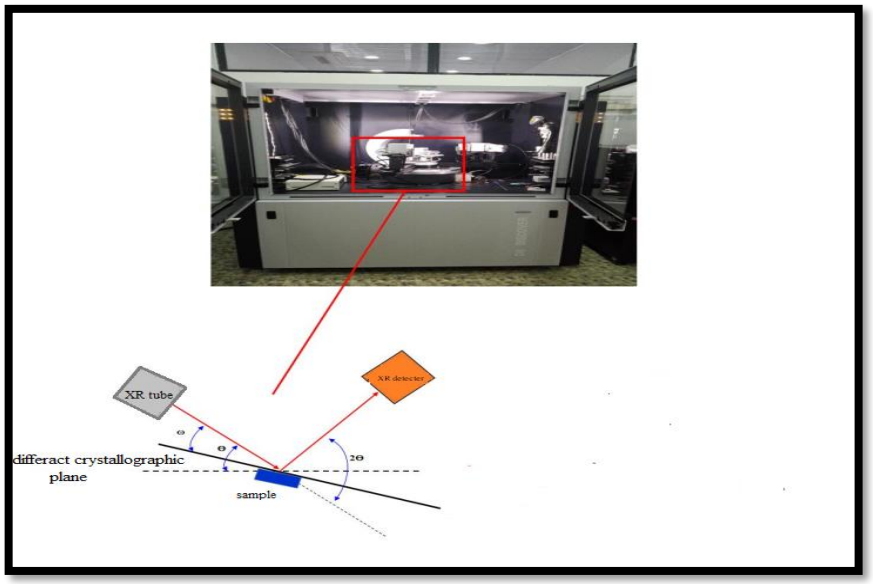

Figure III-15. X-ray diffractometer, Siemens model (BRUKER D8 DISCOVER).

III.5.3 Scanning electron microscope

Scanning electron microscopy (SEM) is a technique that produces images of a sample by scanning it with a beam of electrons. The electrons interact with the different atoms presented at the sample surface, producing various signals that reveal information on the sample surface

morphology and composition. Scanning electron microscopy (SEM) is the most important technique for the analysis of morphological characteristics like size and shape. However, an important limitation of these techniques is the need of high vacuum or ultra-high vacuum conditions, not allowing measurements in an environment as close as possible to real cell operation conditions [53].The schematic of an SEM is shown in figure III-16.

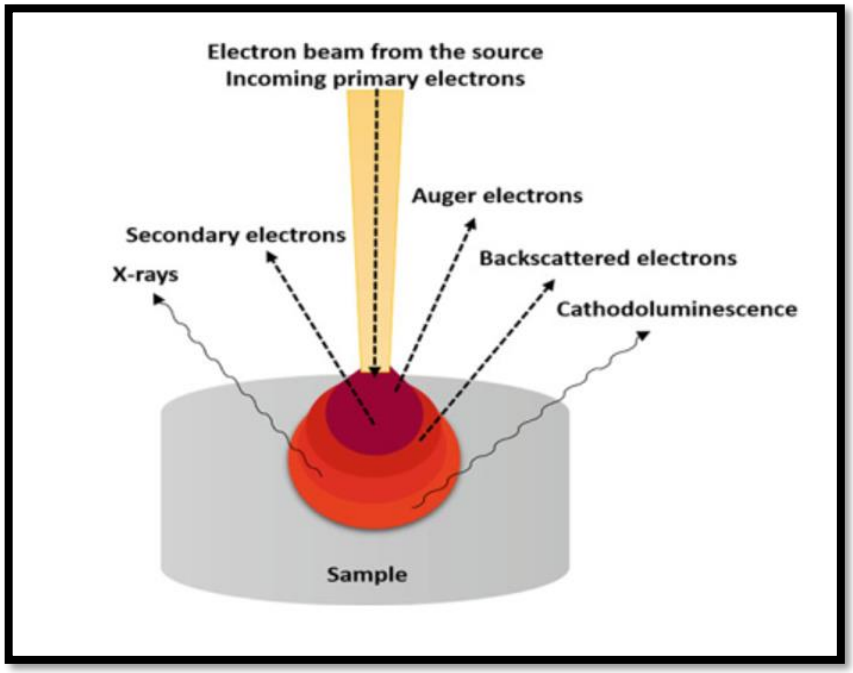

Figure III- 16. The interaction of electron beam with specimen and the signal emitted from the sample [54].

Accelerated electrons in an SEM carry significant amounts of kinetic energy, and this energy is dissipated as a variety of signals produced by electron-sample interactions when the incident electrons are decelerated in the solid sample. The signals are gathered by electron collectors (detectors), which are then manipulated by the computer to form the required image. According to the detected signal (secondary electrons, backscattered electrons or X-rays). The two routinely used electrons for sample image creation are the backscattered and secondary electrons. However, secondary electrons are considered the most important electrons, indicating sample morphology and topography, while backscattered electrons are used for demonstrating the contrasts in multiphase samples composition. SEM is non-destructive, as the generation of X-rays does not lead to any loss in the volume of the specimen; therefore, one can repeatedly analyze the same material (Figure III-17) [54].

In this study, the samples were analyzed by scanning electron microscope (SEM) (Zeiss Gemini SEM 300) equipped with an energy dispersive spectroscopy (EDS) detector as shown in Figure III-17.

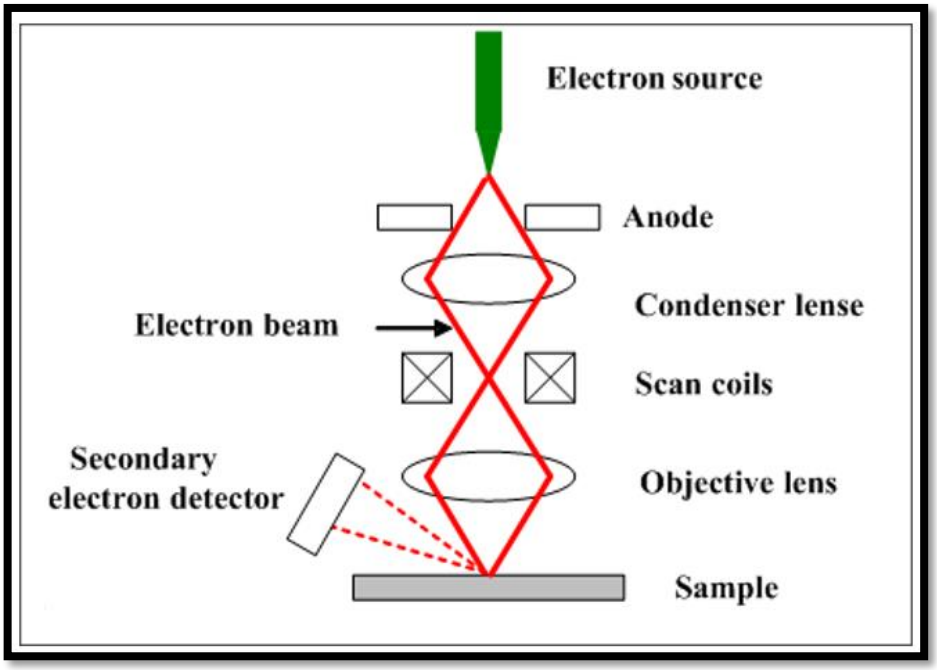

Figure III-17. A principle of scanning electron microscopy [52].

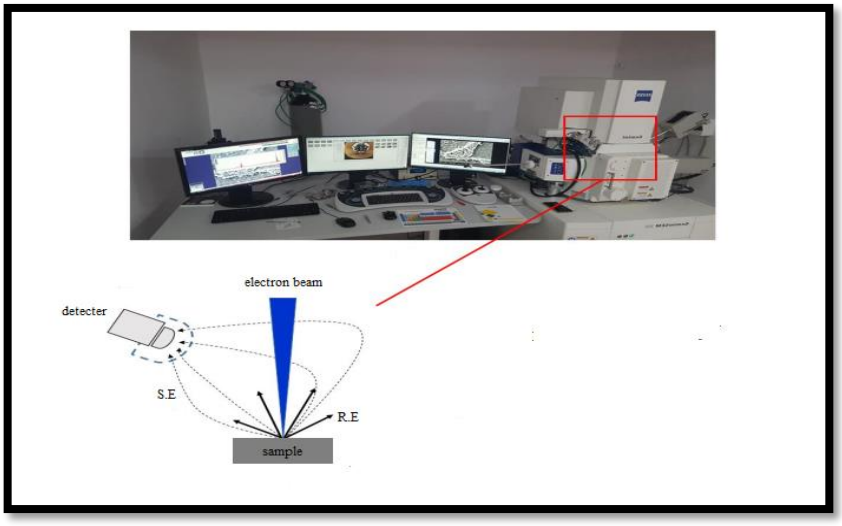

Figure III-18 Scanning Electron Microscope (Zeiss Gemini SEM 300).

III.5.4 Hardness measurements

Hardness measurements were performed by using Hardness tester (Type: INNOVATEST) with load of 2 Kg (Fig.III-19). Hardness profile was performed across the welded joint of the steel.

Figure III-19. Hardness tester (Type: INNOVATEST).

References:

[52] Vilaca P., Friction surfacing.Surface modification by solid stateprocessing, 2014, 25-72.

[53] Gandra J., Miranda R. M . , Vilaca P. , Performance analysis of friction surfacing. Journal of Materials Processing Technology Volume 214, Issue 5, May 2014, Pages 1062-1093

[54] Nicholas E. D. Friction processing technologies. Roissy:International Institute of Welding; 1963

CHAPTER VI
RESULTS AND DISCUSSION

Introduction

The objective of this chapter is to present the results of the effect of the welding process on low carbon steel. Arc welding and laser welding were used as processes of joining the sheets of low carbon steel. The results are explained and discussed.

IV.1 . Base material

IV.1.1 Microstructure

In this study, the used steel is a low carbon steel which its microstructure is presented in Figure IV.1. The structure of the hot-rolled base metal of BS2 steel (0.15 % C) shown two phases one as a matrix and the second as a secondary phase. From the Fe-Fe3C diagram we result that the microstructure is ferrite as matrix and perlite (alternating plates of ferrite and cementite). Some ferrite grains are slightly elongated in the rolling direction. This result is confirmed by SEM shown in Figure IV.2. it shown a polygonal ferrite and pearlite. Polygonal Ferrite forms at the highest austenite transformation temperature and slowest cooling rates in low carbon steels.

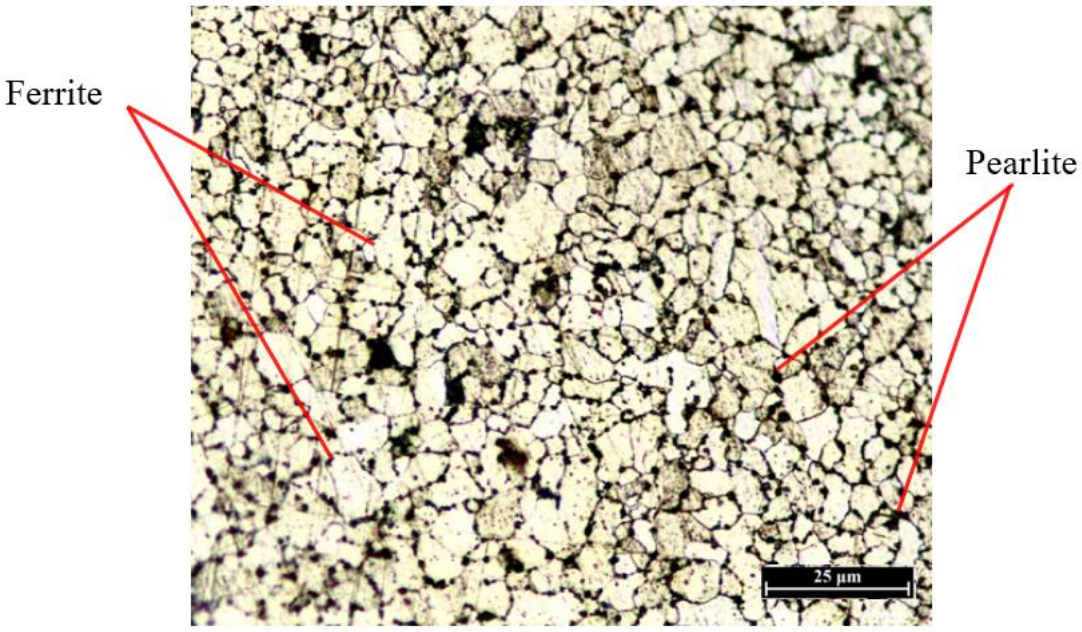

Figure IV.1. Microstructure of BS2 low carbon steel.

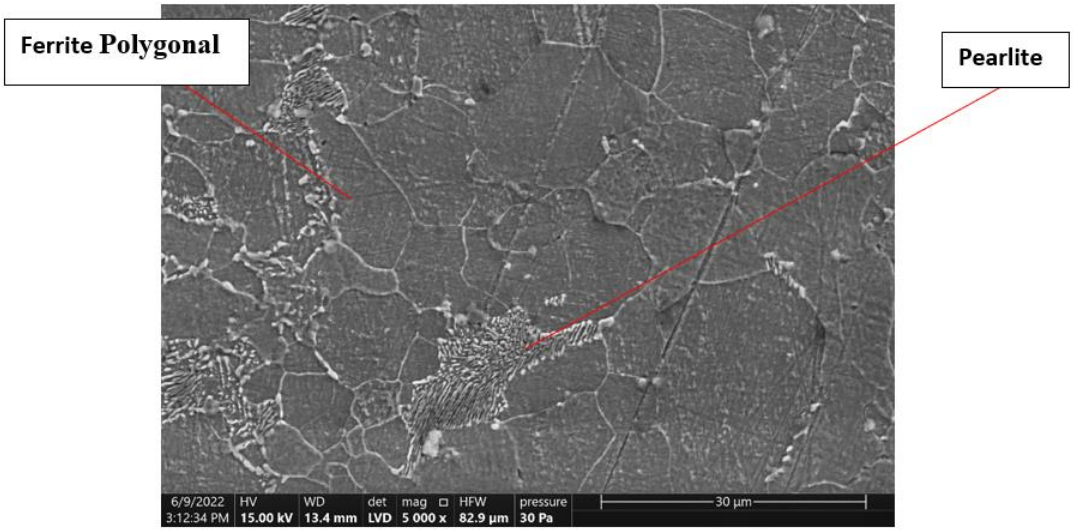

Figure VI.2. Scanning electron micrographs showing distribution and morphology of the basic metal.

IV.1.2 X-ray diffraction

X-Ray diffraction of the base metal in order to know the main phases in basic metal, XRD diffraction was particularly applied in this region (Figure VI.3). From three ferrite peaks observed in this spectrum: the bcc (110), bcc (200) and bcc (211), we conclude a presence only of ferrite phase observed by optical microscopy and SEM.

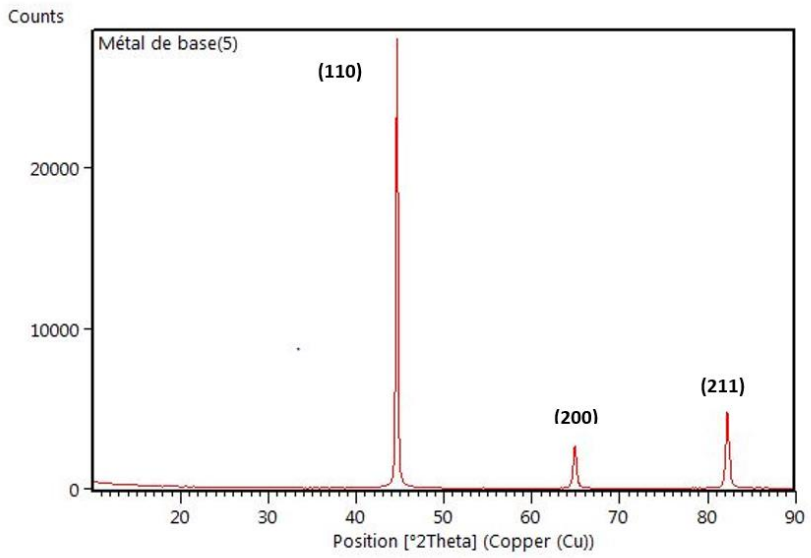

Figure VI.3. XRD spectrum of the BS2 low carbon steel.

IV.2 TIG welding of low carbon steel.

IV.2.1 . Microstructure

Figure IV.4 presents the micrographic views of the TIG welded low carbon steel. The zones were observed:

- Base metal zone (Fig IV.4.a).
- Heat affected zone (Fig IV.4.b).
- Fusion zone (Fig IV.4.c).

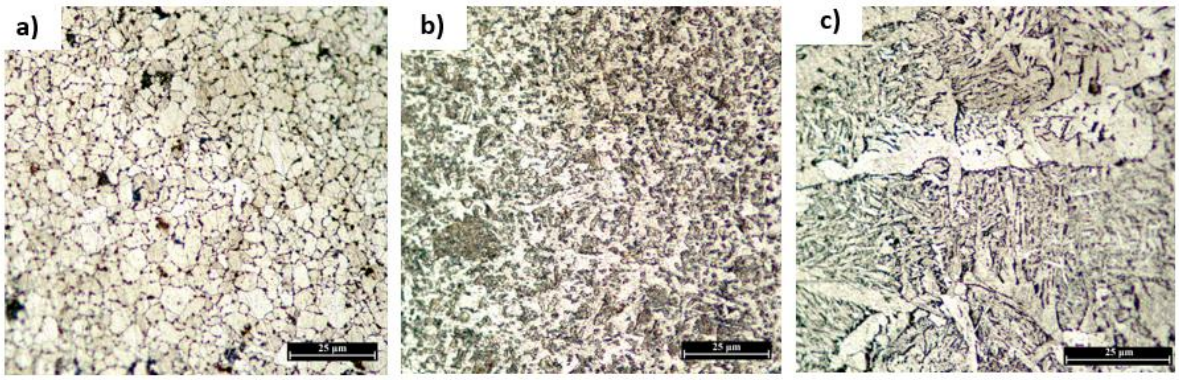

Figure IV.4. Microstructure of deferent zones of the TIG welded low carbon steel

In this part, the microstructures of the three different zones in welded joint will be presented.

IV.2.1.1 Basic metal

The basic metal zones in the TIG welded joint are present in the Figure IV.1.A, it was already discussed at the beginning of this chapter.

IV.2.1.2 Heat affected zone

Figure VI.5 presents the microstructure of the heat affected zone in TIG welded joint. The microstructure of this zone is formed with Ferrite as matrix with pearlite. However, the grain size of ferrite is less than the grain size in the basic metal and this is clearly shown in figure, it is due to the recrystallization reaction caused by the short heat during the welding process. We notice that the plats were submitted a plastic deformation by a hot rolling process

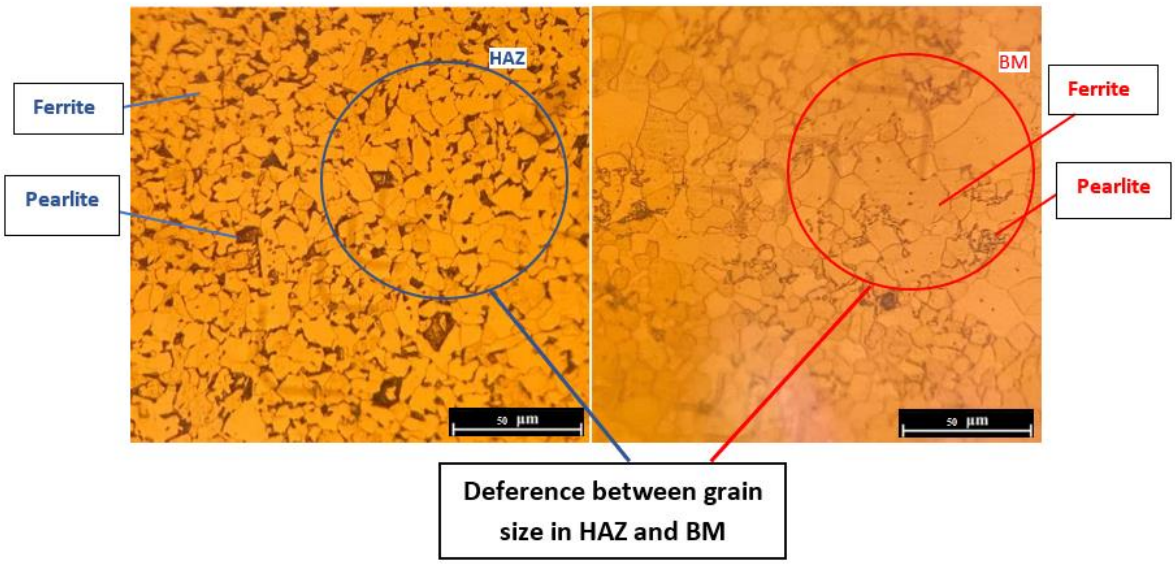

Figure VI.5. Difference of grain size basic metal and heat affected zone in TIG welded steel.

Figure VI.6 present the SEM micrography of the HAZ in the welded joint. The microstructure of the HAZ has submitted a transformation compared to the base metal.

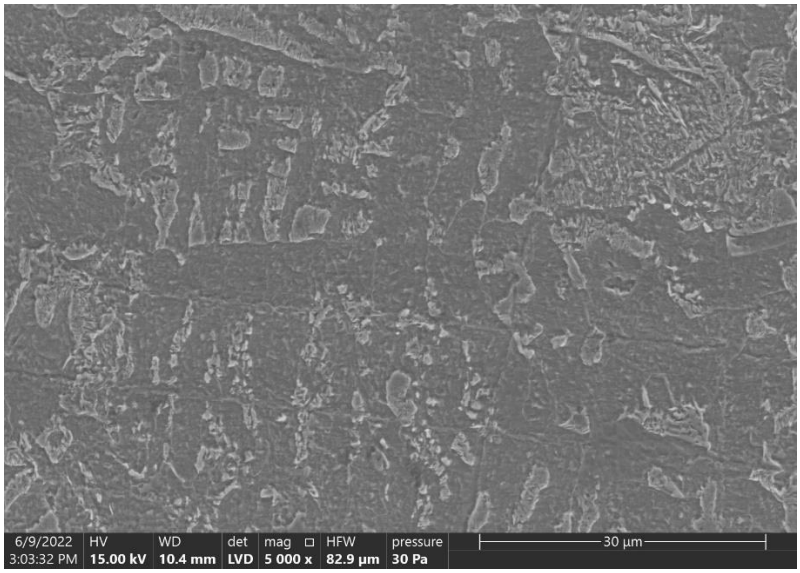

Figure VI.6. Scanning electron micrographs showing distribution and morphology of the heat affected zones of the TIG welded joint.

IV.2.1.3 Fusion zone

Concerning the fusion zone Figure IV.1.b illustrates clearly the microstructures of this zone. It is a mixture of Widmanstatten and acicular ferrite, and some pearlite. Widmanstätten Ferrite has a coarse, elongated morphology and occurs in the form of side plates or laths.WF forms at faster cooling rates and at temperatures just below those at which polygonal ferrite forms. Howevre, acicular ferrite has a lath structure. This type of ferrite forms at high cooling rates in the intermediate temperature transformation range [55].

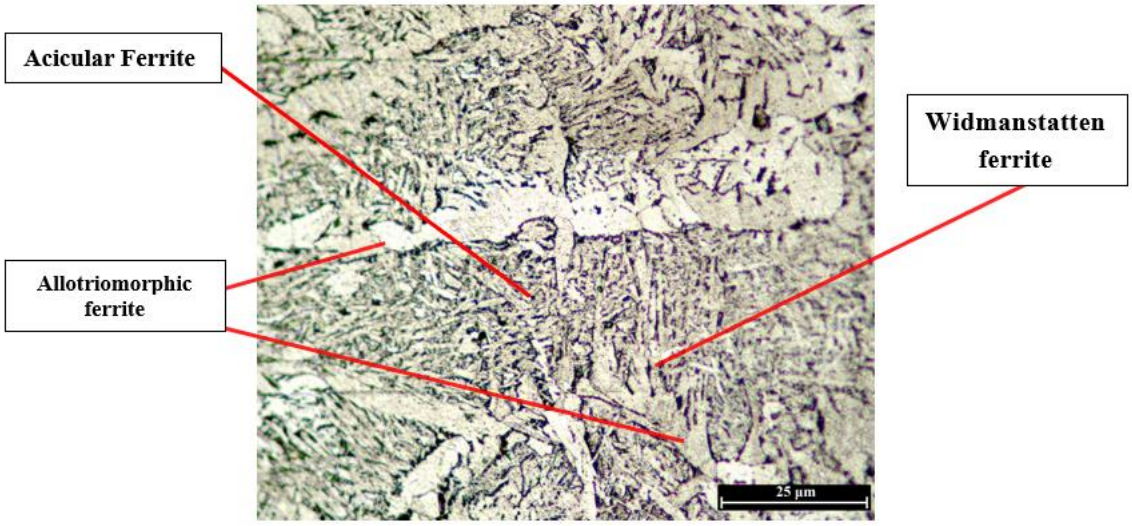

Figure VI.7. Microstructure of the fusion zones of the TIG welded joint.

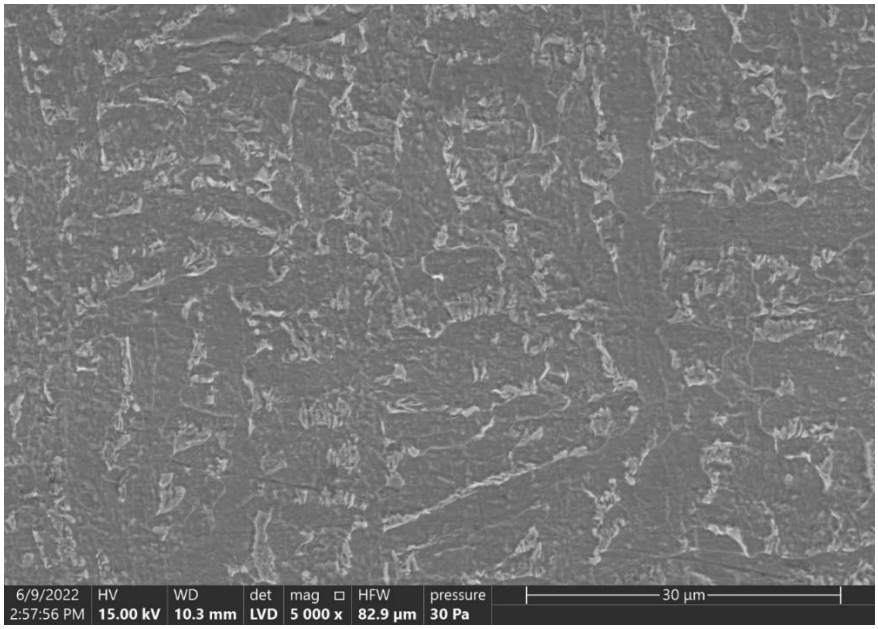

Figure VI.8. Scanning electron micrographs showing distribution and morphology of fusion zone of the TIG welded joint.

IV.2.2 X-RAY diffraction

Figure VI.9 presents the XRD diffractogram of the welded joint by a TIG process. As it is observed there is not a difference between the diffractogram of the base metal and the welded joint, because the same peaks (ferrite peaks) were revealed.

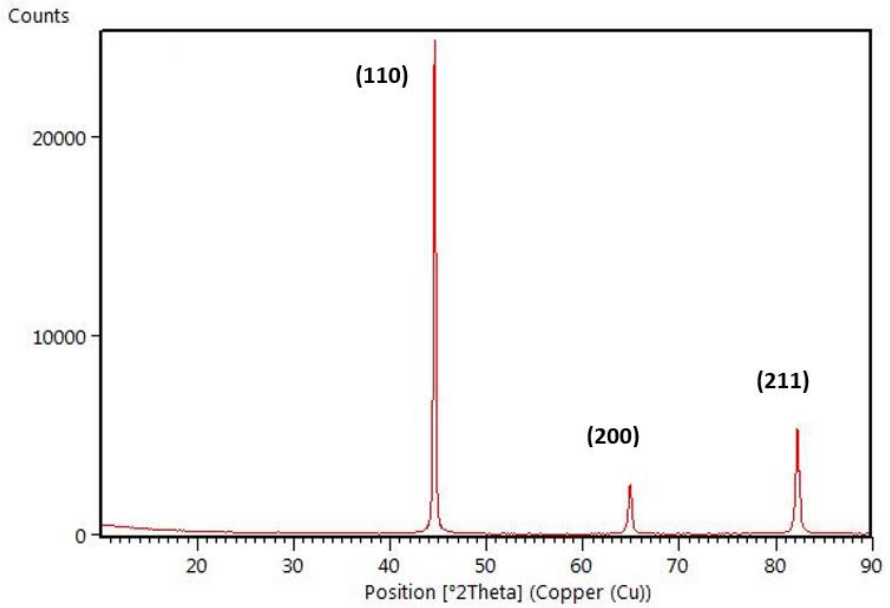

Figure VI.9. XRD diffractogram of the welded joint of low carbon steel.

IV.2.3 Hardness of the TIG welded joint

Microhardness of the base metal was about 144.5 HV (yellow zone in figure VI.10). Distribution of microhardness values in the weld metal was extremely heterogeneous (figure .VI.10). They were significantly higher compared to the base metal. Mean values of microhardness in HAZ increased up to 220.68-220.86 HV (purple zone in figure VI.10) due to the recrystallized fine grain. The microhardness values in FZ decreased down to 180.69 -184.46 HV in FZ (green zone in figure VI.10). The average micro-hardness of the FZ decreases because of the change in cooling rate with increasing welding current, The results obtained are similar to the work of other researchers Kumar, P and al [56].

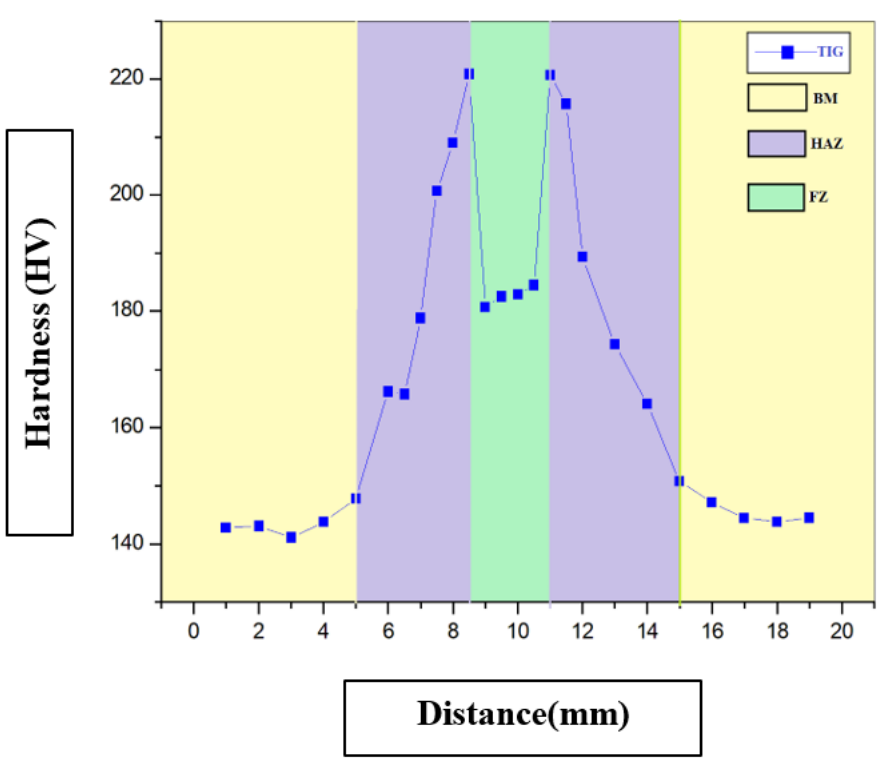

Figure VI.10. Microhardness of the welded metal.

IV.3 Laser welding of low carbon steel

IV.3.1 Microstructure of the welded joint

Figure IV.11 presents the three main zones of the welded joint, base metal (Fig IV.11.a), heat affected zone (Fig IV.11.b), and fusion zone (Fig IV.11.c).

From these microstructures, it can be concluded that the grain size decreases from the base metal to the fusion zones. This phenomenon is due to the heat effect during the laser process.

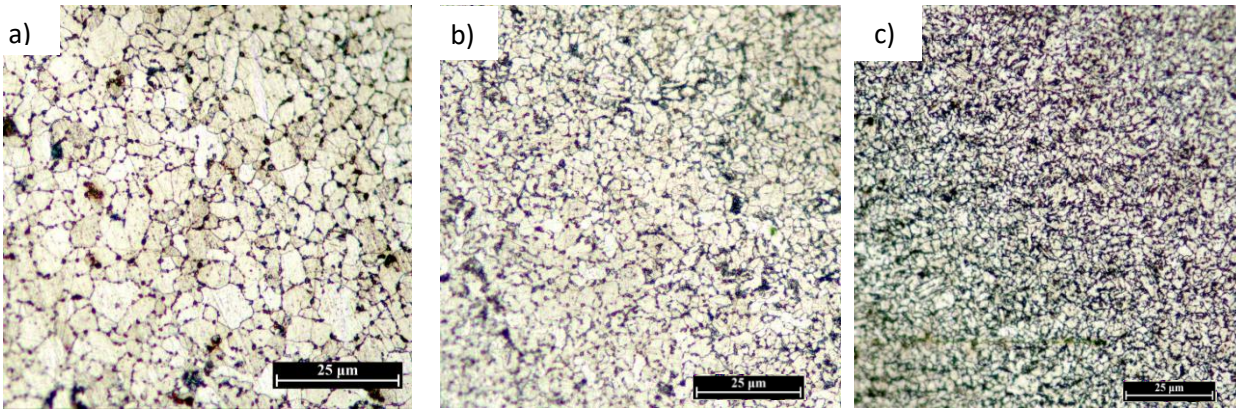

Figure IV.11. Microstructures of different zones of the laser welded low carbon steel.

IV.3.2 . SEM observations of the heat affected zone and fusion zone

Figure IV.12 presents the SEM microstructures of the HAZ (Fig IV.12. a) and the FZ (Fig IV.12. b). From these microstructures, there is a difference between the HAZ and FZ in terms of grain size. The grain size of the FZ (~7µm) is less than the HAZ (~15µm). In addition. More quantity of pearlite is observed in FZ.

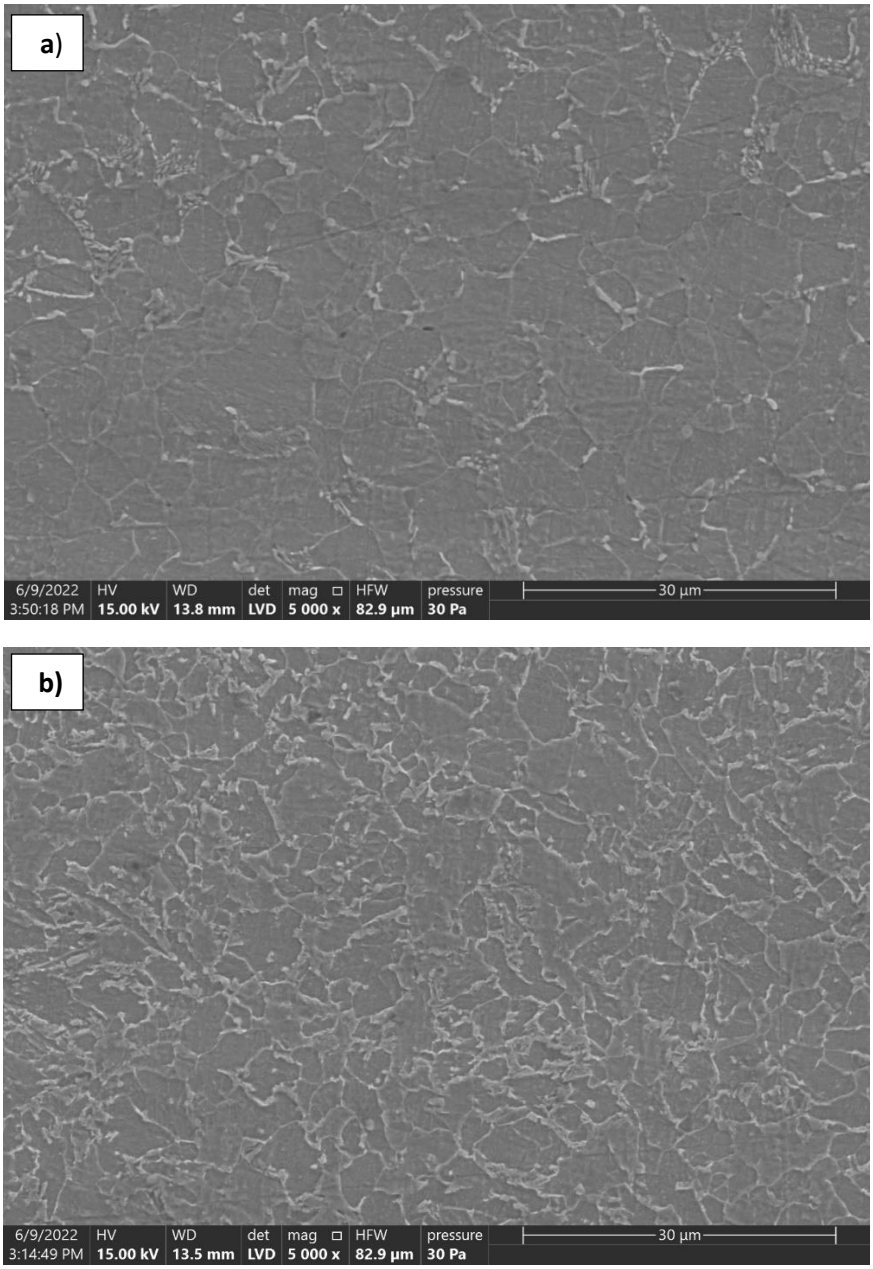

Figure VI.12. SEM observation of the welded joint of the low carbon steel: a) HAZ and b) FZ.

IV.3.3 X-RAY diffraction of Laser welding

Figure VI.13 present the XRD diffraction of the welded joint by laser process. The main three peaks related to the ferrite phase were revealed. However, the industry of these three peaks are more higher than the formed in welded joint by TIG process. This is due to the small grain size in welded joint by laser process.

From the mechanical aspect, the finer grain improves the mechanical properties of the welded joint. consequently, the laser welding process is better than the TIG process for this low carbon steel.

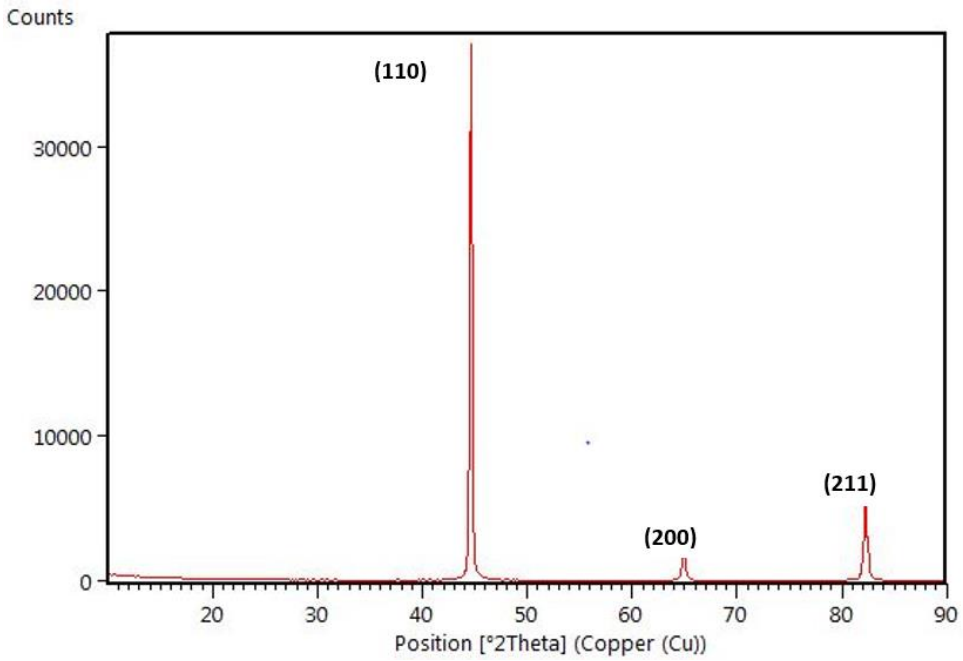

Figure VI.13.XRD diffractogram of the welded joint of low carbon steel by laser process.

IV.3.4 Hardness of the laser welded joint

Figure VI.14 shows the hardness profil curve a cross the laser welded joint of low carbon steel. Distribution of microhardness values in the weld metal was extremely heterogeneous. They were significantly higher compared to the base metal. Mean values of microhardness in FZ increased up to 255.70- 260.32 HV in the HAZ zone (blue zone in figure VI.14). The microhardness values in HAZ up to 180,69 HV (red zone in figure VI.14).

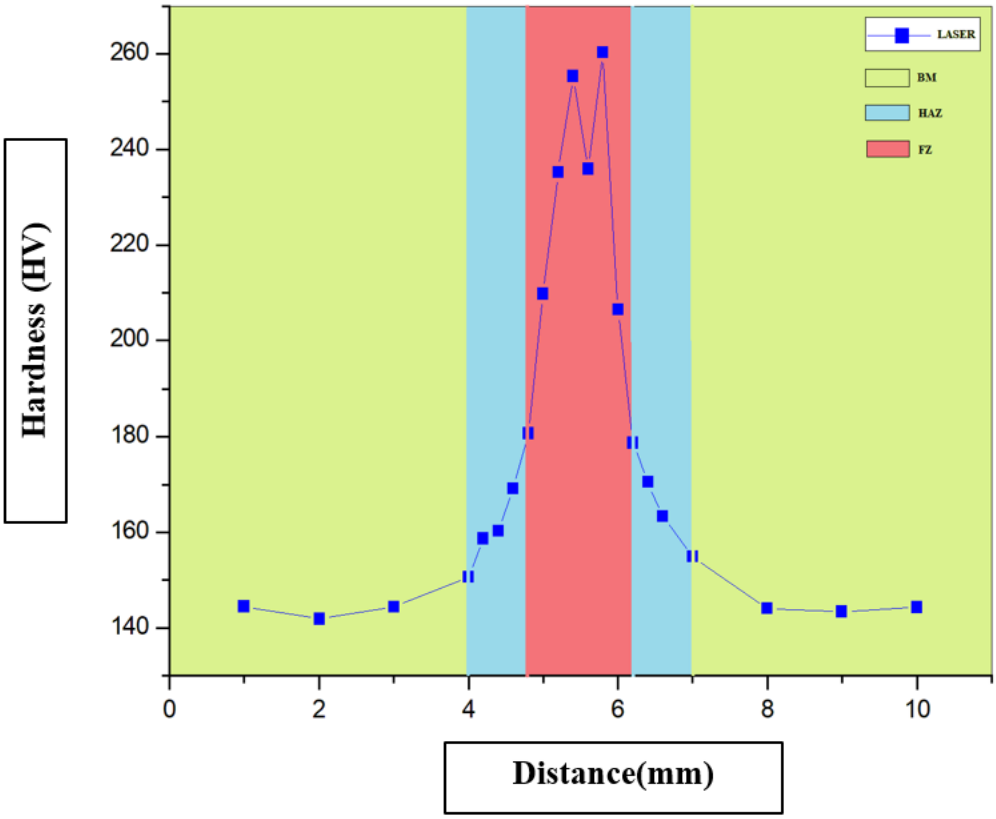

Figure VI.14. Microhardness of the laser welded metal.

Reference

[55] Xiong, Z. P., Kostryzhev, A. G., Stanford, N. E., & Pereloma, E. V. (2015). Microstructures and mechanical properties of dual phase steel produced by laboratory simulated strip casting. Materials & Design, 88, 537-549.

[56] Kumar, P., Sinha, A. N., Hirwani, C. K., Murugan, M., Saravanan, A., & Singh, A. K. (2021). Effect of welding current in TIG welding 304L steel on temperature distribution, microstructure and mechanical properties. *Journal of the Brazilian Society of Mechanical Sciences and Engineering*, *43*(7), 1-20.

General Conclusion

The objective of this study was the investigation of the effect of the welding process on low carbon steel. TIG welding and laser welding were the two joining processes. To achieve our objective four main techniques of characterization were used which are:

- optical microscopy.
- scanning electron microscopy.
- X-Ray Diffraction.
- hardness measurements.

Based on our results, the main following results were obtained:

- The three main zones (BM, HAZ, FZ) were observed in the welded joint by the two processes.
- The hardness values in welded joint have confirmed the difference between the three zones from the microstructural aspect.
- The welded joint by laser welding is formed with finer grains than the welded joint by TIG process. This is confirmed by XRD.
- The welded joint by laser welding is different from the welded joint by TIG process in terms of hardness.

Future work: it will be interesting to study the effect of heat treatment on microstructural and mechanical properties of the welded joints.

ملخص

في هذه المذكرة ، تم لحام الفولاذ منخفض الكربون بواسطة التلحيم القوس الغازي والليزر. يستخدم هذا الفولاذ في صناعة خزانات وقود غاز البترول المسال للسيارات. لتحقيق هدفنا تم استخدام أربع تقنيات رئيسية هي: الفحص المجهري الضوئي ، المسح المجهري الإلكتروني ، قياس الصلادة وانحراف الأشعة السينية ، وجدنا فرقًا مجهريا دقيقًا وميكانيكيًا بين الوصلات الملحومة.

الكلمات المفتاحية : التلحيم بالليزر، التلحيم بالقوس الغازي ، فولاذ .

Résumée

Dans ce mémoire, un acier à bas pourcentage de carbone a été soudé par TIG et laser. Cet acier est utilisé pour la fabrication de réservoirs de GPL pour voitures. Pour atteindre notre objectif, quatre techniques principales ont été utilisées : la microscopie optique, la microscopie électronique à balayage, la mesure de la dureté et la diffraction des rayons X. Nous avons trouvé une différence microstructurale et mécanique entre les joints soudés.

Mots-clés : soudage laser, soudage TIG, acier a faible pourcentage de Carbon.

Abstract

In this dissertation, a low carbon steel was welded by TIG and laser welding. This steel is used for manufacturing of car GPL storage tanks. To achieve our objective, four main techniques were used: optical microscopy, scanning electron microscopy, hardness measurement, and X-RAY diffraction. We have found a microstructural and mechanical difference between the welded joints.

Keywords: Laser welding, TIG welding, low carbon steel.